Geochemistry of hydrothermal fluids from the eastern sector of the Sabatini Volcanic District (central Italy)

D. Cinti [a, *], F. Tassi [b, d], M. Procesi [a], L. Brusca [c], J. Cabassi [b, d], F. Capecchiacci [b, d], A. Delgado Huertas [e], G. Galli [a], F. Grassa [c], O. Vaselli [b, d], N. Voltattorni [a]

[a] Istituto Nazionale di Geofisica e Vulcanologia (INGV), via di Vigna Murata 605, 00143 Roma, Italy
[b] Dipartimento di Scienze della Terra, Università di Firenze, via G. La Pira 4, 50121 Firenze, Italy
[c] Istituto Nazionale di Geofisica e Vulcanologia (INGV), via Ugo La Malfa 153, 90146 Palermo, Italy
[d] CNR - Istituto di Geoscienze e Georisorse, via G. La Pira 4, 50121 Firenze, Italy
[e] Instituto Andaluz de Ciencas de la Tierra IACT (CSIC-UGR), avenida de las Palmas 4, 18100 Armilla, Granada, Spain

ARTICLE INFO

ABSTRACT

This study reports a complete geochemical dataset of 215 water and 9 gas samples collected in 2015 from thermal and cold discharges located in the eastern sector of the Sabatini Volcanic District (SVD), Italy. Based on these data, two main aquifers were recognized, as follows: 1) a cold Ca-HCO_3 to Ca(Na)-HCO_3 aquifer related to a shallow circuit within Pliocene-Pleistocene volcanic and sedimentary formations and 2) a deep CO_2-pressurized aquifer hosted in Mesozoic carbonate-evaporitic rocks characterized by a Ca-$HCO_3(SO_4)$ to Na(Ca)-$HCO_3(Cl)$ composition. A thick sequence of low-permeability formations represents a physical barrier between the two reservoirs. Interaction of the CO_2-rich gas phase with the shallow aquifer, locally producing high-TDS and low-pH cold waters, is controlled by fractures and faults related to buried horst-graben structures. The $\delta^{18}O$-H_2O and δD-H_2O values indicate meteoric water as the main source for both the shallow and deep reservoirs. Carbon dioxide, which is characterized by $\delta^{13}C$-CO_2 values ranging from −4.7 to +1.0‰ V-PDB, is mostly produced by thermo-metamorphic decarbonation involving Mesozoic rock formations, masking possible CO_2 contribution from mantle degassing. The relatively low R/R_a values (0.07−1.04) indicate dominant crustal He, with a minor mantle He contribution. The $CO_2/^3He$ ratios, up to 6×10^{12}, support a dominant crustal source for these two gases. The $\delta^{34}S$-H_2S values (from +9.3 to +11.3‰ V-CDT) suggests that H_2S is mainly related to thermogenic reduction of Triassic anhydrites. The $\delta^{13}C$-CH_4 and δD-CH_4 values (from −33.4 to −24.9‰ V-PDB and from −168 to −140‰ V-SMOW, respectively) and the relatively low C_1/C_{2+} ratios (<100) are indicative of a prevailing CH_4 production through thermogenic degradation of organic matter. The low N_2/Ar and high N_2/He ratios, as well as the $^{40}Ar/^{36}Ar$ ratios (<305) close to atmospheric ratio, suggest that both N_2 and Ar mostly derive from air. Notwithstanding, the positive $\delta^{15}N$-N_2 values (from +0.91 to +3.7‰ NBS air) point to a significant extra-atmospheric N_2 contribution. Gas geothermometry in the CH_4-CO_2-H_2 and H_2S-CO_2-H_2 systems indicate equilibrium temperatures <200 °C, i.e. lower than those measured in deep geothermal wells (~300 °C), due to either an incomplete attainment of the chemical equilibria or secondary processes (dilution and/or scrubbing) affecting the chemistry of the uprising fluids. Although the highly saline Na-Cl fluids discharged from the explorative geothermal wells in the study area support the occurrence of a well-developed hydrothermal reservoir suitable for direct exploitation, the chemistry of the fluid discharges highlights that the uprising hydrothermal fluids are efficiently cooled and diluted by the meteoric water recharge from the nearby Apennine sedimentary belt. This explains the different chemical and isotopic features shown by the fluids from the eastern and western sectors of SVD, respectively, the latter being influenced by this process at a lesser extent. Direct uses may be considered a valid alternative for the exploitation of this resource.

* Corresponding author.
    E-mail address: daniele.cinti@ingv.it (D. Cinti).

1. Introduction

The Sabatini Volcanic District (SVD) is part of the peri-Tyrrhenian sector of central Italy, an area characterized by a complex geodynamic setting that, during the Neogene, produced NNW-SSE oriented horst-graben structures, alkaline magmatism, and a widespread thermal anomaly (Barberi et al., 1994, Fig. 1). In this region, mantle degassing and thermo-metamorphic processes feed a regional pressurized gas system (e.g., Chiodini et al., 1999; Minissale, 2004) that is connected to CO_2-rich thermal and cold fluid discharges through fractures and faults related to an extensional tectonic regime (Barberi et al., 1994), producing a number of CO_2-rich thermal and cold fluid discharges.

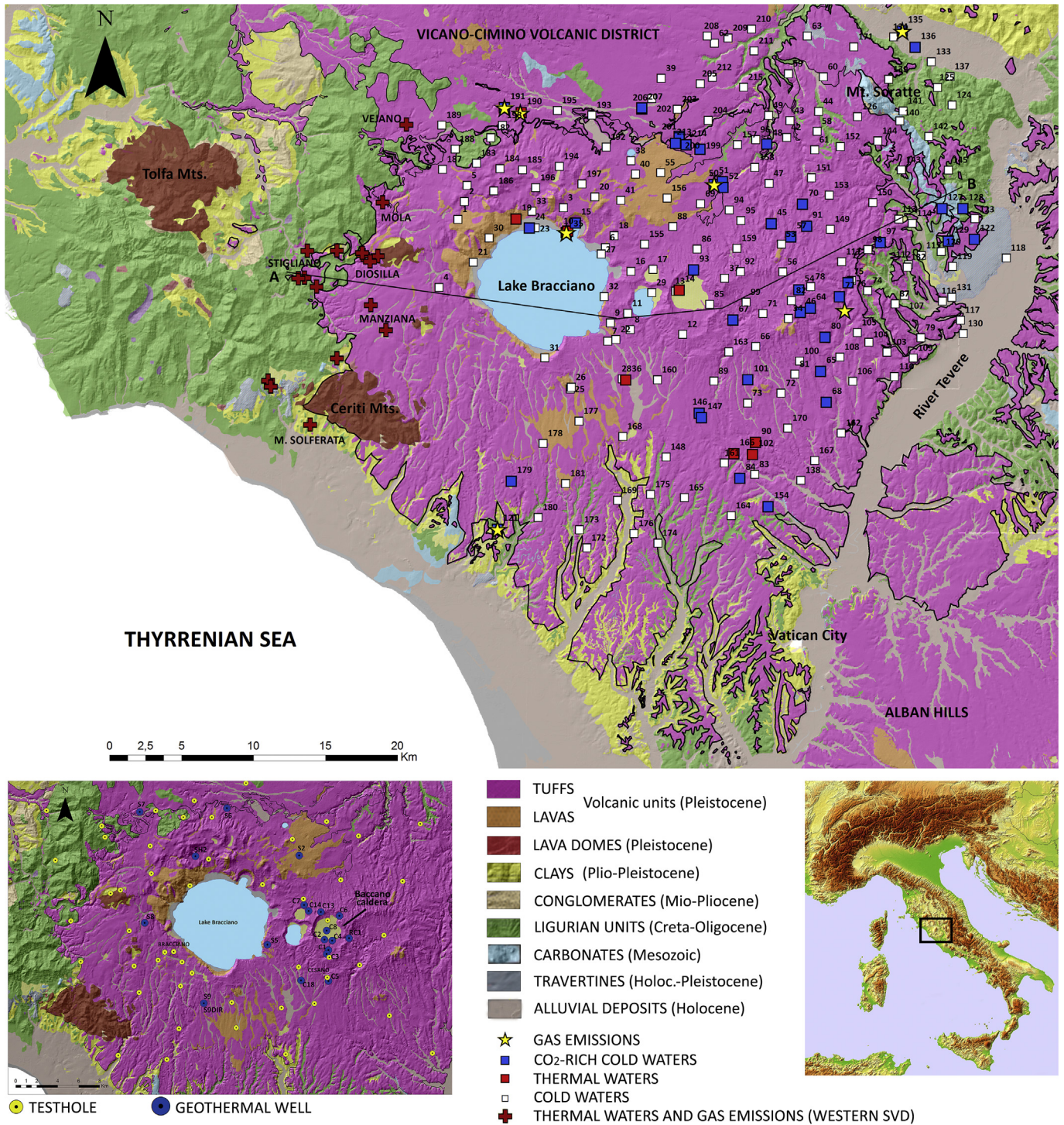In the framework of exploration surveys carried out in the past

Fig. 1. Geological sketch map of the Sabatini Volcanic District (SVD) showing the location of the fluid sampling sites. Location of natural gas emission in western SVD are taken from Cinti et al. (2011). Location of test-holes and geothermal wells are from Buonasorte et al. (1991) and http://unmig.mise.gov.it/unmig/geotermia/pozzi/pozzi.asp, respectively. Interpretative section corresponding to trace A-B is reported in Fig. 14.

decades for geothermal exploitation purposes (Calamai et al., 1976; Funiciello et al., 1979; Allegrini et al., 1982; Cavarretta and Tecce, 1987; Buonasorte et al., 1995), a high enthalpy geothermal field was recognized in the eastern SVD (i.e. Cesano field; Calamai et al., 1976). Explorative wells (from 960 to 3200 m depth) were drilled within the Baccano Caldera (Fig. 1; Funiciello et al., 1979), where a maximum temperature of ~300 °C was measured (Allegrini et al., 1982). Potentially productive wells (C1, C5, C7, C8), having an average depth of ~1750 m and bottom-hole temperatures ranging from 141 to 221 °C, discharged a highly saline (up to 350 g/L) brine associated with a CO_2-dominated gas phase (Calamai et al., 1976). Due to the high salinity of the liquid phase and the relatively high concentrations of corrosive gases (H_2S), these wells were considered not economically exploitable and then abandoned (Billi et al., 1986). Few years later, the geothermal exploration resumed in this area and new wells were drilled outside the Baccano Caldera (Fig. 1; Cavarretta and Tecce, 1987; Buonasorte et al., 1991, 1995). Among them, 8 wells (from 1390 to 3886 m depth) were drilled within the SVD, where bottom-hole temperatures up to 300 °C were measured. Nevertheless, the hydrothermal resource was not considered economically exploitable. Notwithstanding these negative attempts, Italy is recently experiencing a renewed interest for geothermal energy, favoured by new technological advances, encouraged by the growth of energy demand and the need to reduce CO_2 emissions to the atmosphere (Procesi et al., 2013). Presently, in the Latium region new research concessions have already been conferred, whereas private companies are claiming other areas for geothermal prospecting purposes (http://unmig.mise.gov.it/unmig/geotermia/titoli/titoli.asp). This provided a new pulse for developing geochemical investigations on thermal fluid discharges in central Italy, including the SVD.

The main geochemical features of the thermal discharges in central Italy were discussed in several studies carried out since the 1970's (e.g., Baldi et al., 1973; Dall'Aglio et al., 1994; Duchi and Minissale, 1995; Chiodini et al., 1999; Minissale et al., 1997a; Minissale, 2004). On a local scale, a geochemical study focusing on the western sector of the SVD (Cinti et al., 2011) reported a detailed chemical and isotopic dataset, which allowed to construct a conceptual model aimed to describe the hydrothermal fluid circulation. In 2015, following a similar approach, the geochemical investigation was extended to fluid discharges from the eastern SVD (Fig. 1). A similar detailed approach was adopted in the present study to complete the description of the hydrothermal fluid circulation related to this volcanic complex. Up to 215 waters and 9 bubbling gases (Fig. 1) were collected and analyzed for determining the composition of the main and trace components and the stable isotopes of water, CO_2 and CH_4, noble gases (He and Ar), N_2, and sulfur in H_2S. The main goals were to: *i*) investigate the fluid sources and the main chemical-physical processes controlling fluid chemistry, *ii*) propose a conceptual model to describe the circulation pattern and the processes controlling the chemistry of the thermal fluids, and *iii*) provide insights into the most promising areas for geothermal exploitation. For these goals, the available stratigraphic, structural, and hydrogeological data were also used.

2. Geological, structural and hydrological setting

The ~1000 km^2 wide study area is located along the peri-Tyrrhenian sector of central Italy (Fig. 1). In this region, a post-collisional tectonic activity occurred during the Neogene, generating dominantly extensional NNW-SSE-trending fault systems (Barberi et al., 1994) and minor NE-SW-trending transtensive structures that accommodated differential extension (Acocella and Funiciello, 2006). The progressive eastward migration of the extension wave produced a strong crustal thinning (<25 km;

Scrocca et al., 2003), high heat flow (locally >200 mW/m^2; Della Vedova et al., 1984; Barberi et al., 1994), and subduction-related magmatism (Peccerillo, 1985; Barberi et al., 1994; Doglioni et al., 1999). Volcanic complexes grew up on buried horst-graben structures, as shown by gravimetric anomalies (Barberi et al., 1994), whilst marine clastic sediments were filled the structural lows.

The SVD was active from 0.60 to 0.08 Ma (Cioni et al., 1993; De Rita et al., 1996; Karner et al., 2001) and consisted of rhyolites, rhyodacites and trachidacites found as dome complexes (Cimarelli and De Rita, 2006), pertaining to the Tuscan Magmatic Province, and under-saturated alkali-potassic pyroclastic and phreato-magmatic deposits with subordinate volumes of lavas related to the Roman Magmatic Province. The early stage of the volcanic activity (0.6–0.4 Ma), mostly consisting of explosive events, occurred from craters located in the eastern and southern sectors of the SVD, while the main explosive phase (0.3 Ma), producing caldera-forming pyroclastic flows and several small scoria cones and tuff rings, took place north of the Bracciano volcano-tectonic depression. During the latest eruptive phase (0.17–0.08 Ma) hydro-magmatic products were ejected from N-S and E-W-oriented craters located along the eastern margin of Lake Bracciano.

The volcanic products overly a tectono-stratigraphic sequence consisting of (from top to bottom): 1) a Plio-Pleistocene complex, including conglomerates, sandstones and clays, 2) Cretaceous-Oligocene (?) Ligurian and sub-Ligurian units (Ligurian s.l.), including calcareous-pelitic calcarenites and arenaceous-pelitic turbidites (Fazzini et al., 1972), 3) Mesozoic carbonates, and 4) Triassic evaporites (Burano Fm.).

The hydrogeological setting is dominated by a regional hydro-thermal reservoir hosted in the carbonate-evaporite units and a shallow, mainly unconfined, regional aquifer within the volcanic rocks (Capelli et al., 2005). Low-permeability Plio–Pleistocene deposits and/or the Ligurian s.l. rocks act as an efficient impervious barrier between the shallow and the deep aquifer. Locally, permeable layers within the low-permeability sedimentary deposits host perched aquifers that feed numerous springs of limited and discontinuous extent (Dall'Aglio et al., 1994). The Bracciano Lake represents the outcrop of the shallow volcanic aquifer. Three piezometric highs, identified near the Bracciano Lake (Capelli et al., 2005), force groundwater to flow towards the Tevere River to the E, the Tolfa Mountains to the W and the lake itself, respectively (Fig. 1).

3. Methods

Water samples were collected from cold and thermal springs, occasionally showing bubbling gases, as well as municipal and domestic wells. The chemical and isotopic dataset also includes published data (Cinti et al., 2014) of 34 waters and 4 bubbling gases (samples 190, 191, 201, 216) located at the border between the SVD and the Vicano-Cimino Volcanic District. The field and laboratory analytical results are listed in Table 1 and as supplementary material (Tables 1S and 2S).

3.1. Groundwater sampling and analysis

Temperature, pH, Eh, electrical conductivity and alkalinity concentrations (acidimetric titration with 0.05 N HCl) concentrations were determined *in situ*. One filtered (0.45 μm) and two filtered and acidified (with ultra-pure HCl and HNO_3, respectively) aliquots were collected and stored in high-density polyethylene bottles for laboratory analysis. Major anions (F^-, Cl^-, Br^-, SO_4^{2-} and NO_3^-) and cations (Ca^{2+}, Mg^{2+}, Na^+ and K^+) were analyzed by ion-chromatography (IC; Thermo Scientific Dionex ICS-900) on filtered and filtered-acidified (HCl) samples, respectively. An unfiltered

Table 1
Chemical and isotopic composition of the gas discharges. Gas contents are in mmol/mol except for Ne, C_2H_6 and C_3H_8 which are expressed in µmol/mol; $\delta^{13}C$ in CO_2 and CH_4 as ‰ V-PDB; δD in CH_4 as ‰ V-SMOW; $\delta^{15}N$ as ‰ NBS air; $\delta^{34}S$ as ‰ V-CDT. Data from samples 190–216 are taken from Cinti et al. (2014).

ID	Site	CO_2	H_2S	N_2	CH_4	Ar	O_2	H_2	He	Ne	C_2H_6	C_3H_8
10	trevignano 1	966	1.10	31	0.37	0.62	0.91	0.0150	0.0006	0.00123	3.5	0.61
50	monte caio	968	0.33	29	0.16	0.55	2.4	0.0080	0.0009	0.00099	7.1	0.80
77	fosso s. antonino	961	2.10	33	1.9	0.75	0.62	0.0190	0.0013	0.00080	66	9.0
121	castel campanile	960		36	2.7	0.71	0.21	0.0160	0.0015	0.00025	78	9.0
135	acqua forte ponzano	966	0.29	32	0.85	0.76	0.39	0.0041	0.0045	0.00067	7.8	0.85
190	mola bassano	993	0.02	6.0	0.35	0.056	0.10	0.0392	0.0003	0.00003	2.1	0.10
191	pian del vescovo	994	0.04	5.1	0.31	0.071	0.09	0.0532	0.0004	0.00004	3.0	0.11
201	terme dei gracchi 2	992	0.08	7.9	0.06	0.133	0.10	0.0085	0.0007	0.00005	0.55	0.02
216	solforate nepi	994	0.43	5.4	0.07	0.049	0.06	0.0160	0.0021	0.00003	0.22	0.01

ID	R/R_a	$^4He/^{20}Ne$	$^{40}Ar/^{36}Ar$	$\delta^{13}C-CO_2$	$\delta^{13}C-CH_4$	$\delta D-CH_4$	$\delta^{15}N-N_2$	$\delta^{34}S-H_2S$	^3He (x 10^{-10})	$CO_2/^3He$ (x 10^{12})
10	0.61	0.49	290.9	0.26	−29.2	−155		9.5	5.1	19
50	0.74	0.94	301.4	−4.73	−30.6	−154		9.7	9.6	10
77	1.04	16.1	297.5	1.02	−33.4	−166		10.3	19	5.1
121	0.07	6.11	293.4	−1.69	−25.2	−160	1.6		1.6	60
135	0.88	6.65	304.9	−0.47	−31.2	−165		10.6	55	1.8
190		0.79		−1.06	−25.1	−147		9.3		
191	0.71	2.23	295.5	−0.04	−24.9	−140		11.3	4.0	25
201	0.69	1.62		−1.93	−28.4	−168	0.91	9.6	6.6	15
216	0.55	1.13		−1.22	−26.3	−149	3.7	9.8	16	6.1

diluted (1:10) sample was collected for the determination of SiO_2 by molecular spectrophotometry (MS). The analytical errors for IC and MS were <5%. An unfiltered sample was collected for the determination of NH_4 by Ion−Selective Electrode method (ISE). The analytical error for ISE was <10%. Minor and trace elements (B, Li, Fe, Mn, Al, Sr) were determined on the filtered-acidified (with HNO_3) samples by inductively coupled plasma mass spectrometry (ICP−MS; Agilent 7500ce). The analytical error for ICP-MS was <10%.

The $^{18}O/^{16}O$ and $^2H/^1H$ ratios of water (expressed as $\delta^{18}O-H_2O$ and $\delta D-H_2O$ ‰ V-SMOW) were determined by isotope ratio mass spectrometry (IRMS). Oxygen isotopes measurements were carried out by using a Gas Bench peripheral coupled with a Thermo Delta V mass spectrometer. A TC-EA peripheral interfaced by means of a ConFloIV with Thermo Delta XP mass spectrometer was used for hydrogen isotopes. The analytical error for IRMS was ±0.1‰ for $\delta^{18}O$ and better than ±1‰ for δD. The $^{13}C/^{12}C$ isotopic ratios of Total Dissolved Inorganic Carbon (TDIC), expressed as $\delta^{13}C$-TDIC ‰ V-PDB, were analyzed by mass spectrometry (Finnigan Delta plus XP) following the procedure described by Salata et al. (2000). The analytical error for MS was ±0.1‰.

3.2. Dissolved and free gas sampling and analysis

Water samples for the determination of dissolved gases were collected in 125 mL glass flasks equipped with a rubber septum. Dissolved gas chemistry (H_2, He, O_2, N_2, CH_4, CO_2, Ne) was determined in the free-gas phase, formed in the headspace of the sampling flasks by injecting Ar through the rubber septum, by gas chromatography (GC) using a Varian CP-4900 Micro gas chromatograph equipped with two TCD detectors and Ar as carrier gas (Capasso and Inguaggiato, 1998). The dissolved gas concentrations (expressed in bar) were calculated from the composition of the headspace gas on the basis of the solubility coefficients of each gas compound (Whitfield, 1978). Analytical error for GC was <5%.

Free gases were collected from bubbling pools by using a plastic funnel positioned above the gas emergence and connected to glass thorion-tapped flasks through a silicon tube. Three gas aliquots were collected, as follows: 1) a pre-evacuated 150 mL glass flask for the determination of $^{13}C/^{12}C$, $^{40}Ar/^{36}Ar$, $^3He/^4He$ and $^4He/^{20}Ne$ isotopic ratios; 2) a pre-evacuated 150 mL glass flask filled with

50 mL of a 4N NaOH solution for the determination of carbon and hydrogen and nitrogen isotopes in CH_4 and N_2, respectively; 3) a pre-evacuated 60 mL glass flask filled with 20 mL of a 5N NaOH and 0.15M $Cd(OH)_2$ suspension for the determination of the chemical composition and $^{34}S/^{32}S$ isotopic ratio in H_2S (Giggenbach and Goguel, 1989; Montegrossi et al., 2001; Vaselli et al., 2006). Low-solubility inorganic gases and CH_4 were analyzed by GC using a Shimadzu 15A gas chromatograph, equipped with a 10 m long 5A molecular sieve column and a thermal conductivity detector (TCD), and a Thermo Focus gas chromatograph equipped with a 30 m long capillary molecular sieve column and a TCD. Light hydrocarbons were determined with a Shimadzu 14A gas chromatograph equipped with a 10 m long stainless steel column ($\phi = 2$ mm) packed with Chromosorb PAW 80/100 mesh coated with 23% SP 1700 and equipped with a FID detector. CdS in the solid precipitate of aliquot (3), formed by the reaction of Cd and H_2S, was separated from the liquid phase by centrifugation at 4000 rpm for 30 min, oxidized to SO_4^{2-} by H_2O_2, and then analyzed by IC (Methrom 761). Carbon dioxide was analyzed as CO_3^{2-} in the alkaline solution by acidimetric titration with 0.1 N HCl. The analytical error for the gas chemical analysis was <10%.

The $^{13}C/^{12}C$ isotopic ratios in CO_2 (expressed as $\delta^{13}C$ ‰ V-PDB) were determined by MS using a Finningan Delta S mass spectrometer, after a two-step extraction and purification procedures of the gas mixtures by using liquid N_2 and a solid-liquid mixture of liquid N_2 and trichloroethylene. Internal (Carrara and San Vincenzo marbles) and international (NBS18 and NBS19) standards were used to estimate external precision. The analytical error and the reproducibility were ±0.05‰ and ±0.1‰, respectively.

The $^{13}C/^{12}C$ and $^2H/^1H$ isotopic ratios in CH_4 (expressed as $\delta^{13}C$ ‰ V-PDB and δD ‰ V-SMOW) were analyzed by mass spectrometry (Varian MAT 250) according to the procedure described in Schoell (1980). The analytical error was ±0.15‰ for $\delta^{13}C$ and ±1‰ for δD. The $^{34}S/^{32}S$ isotopic ratios in H_2S (expressed as $\delta^{34}S$ ‰ V-CDT) were determined after the precipitation of SO_4^{2-}, produced by the oxidation of CdS precipitated in the aliquot (3), as $BaSO_4$ by adding a $BaCl_2$ solution (10% w/v). Sulfur isotopes in H_2S were analyzed by using an EA-IRMS system consisting of a 20-20 isotope ratio mass spectrometer (Europa Scientific, Crewe, UK), equipped with an elemental analyzer (Sercon Ltd., Crewe, UK). The analytical error was <0.3‰. Nitrogen isotopes in N_2 (expressed as $\delta^{15}N$ ‰ NBS air)

were determined with an Agilent 6890N gas-chromatograph coupled to a Finnigan Delta plus XP mass spectrometer. Helium isotopic ratios (expressed as R/R_a, where R is the $^3He/^4He$ measured ratio and R_a is the $^3He/^4He$ ratio in the air: 1.39×10^{-6}; Mamyrin and Tolstikhin, 1984), as well as the $^4He/^{20}Ne$ and $^{40}Ar/^{36}Ar$ ratios, were analyzed by a GVI Helix SFT mass spectrometer after gas samples purification in the high-vacuum inlet line of the instrument (Rizzo et al., 2015). The analytical error in the determination of elemental He and Ne contents was <5%.

4. Results

4.1. Chemical and isotopic composition of waters

Cold waters from both the volcanic and sedimentary domains (Fig. 1) are characterized by low Total Dissolved Solids (TDS) values (<1000 mg/L), slightly acidic-to-alkaline pH values (from 6.3 to 8.0) and Ca-HCO$_3$ to Ca(Na)-HCO$_3$ chemical composition (Fig. 2a and b). Exceptions are a significant number of cold waters, locally known as *acque acetose* (samples 15, 24, 45, 46, 48, 50, 51, 52, 57, 64, 68, 70, 75, 77, 80, 84, 91, 97, 101, 122, 127, 128, 129, 135, 136, 146, 147, 154, 179, 199, 200, 201, 207, 213, 214), which are characterized by relatively high TDS (up to 4014 mg/L) and lower pH values (from 5.2 to 6.7). Relatively few cold waters show a Ca-SO$_4$ composition (samples 54, 65, 67, 93, 121, 191 and 206) and have variable TDS (from 239 to 3827 mg/L) and pH (from 3.1 to 6.7) values. The concentrations of minor and trace elements are marked by a large variability, as follows: Li from 0.005 to 0.80 mg/L, B from 0.02 to 6.8 mg/L, Al from 0.005 to 78 mg/L, Mn from 0.005 to 5.5 mg/L, Fe from 0.005 to 112 mg/L, Sr from 0.08 to 6.8 mg/L.

Thermal waters (from 22.5 to 61.5 °C) have relatively high TDS values (from 1179 to 4035 mg/L), with the exception of sample 190 (493 mg/L), and slightly acidic pH (from 5.2 to 6.6). They show a Ca-HCO$_3$(SO$_4$) to Na(Ca)-HCO$_3$(Cl) composition (Fig. 2a and b), and concentrations of Li, B, Fe, Al, Mn and Sr, are marked by a large variability (49–1424, 211 to 8161, 0.71 to 7156, 3.3 to 176, 0.32–827 μg/L and 0.23–9.2 mg/L, respectively).

The δ^{18}O-H$_2$O and δ^{2}H-H$_2$O values range from −7.1 to −4.7‰ and from −44 to −30‰ V-SMOW, respectively (Table 1S), with no significant difference between cold and thermal waters, with the exception of sample 121, associated with bubbling gases, that can be distinguished by a strongly negative δ^{18}O-H$_2$O and δ^{2}H-H$_2$O values (−14.9 and −27‰ V-SMOW, respectively).

The δ^{13}C-TDIC values range from −21.2 to +5.39‰ V-PDB

(Table 2S).

4.2. Chemical and isotopic composition of dissolved gases

The dissolved gases mainly consist of atmospheric compounds (N$_2$ and O$_2$), whose partial pressures are up to 0.98 and 0.20 bar, respectively. The pCO$_2$ values are low (<0.038 bar) in the cold bicarbonate-type waters (Table 2S) and significantly higher in *acque acetose* (up to 0.35 bar), in SO$_4$-rich cold waters (up to 0.36 bar) and thermal waters (up to 0.27 bar). The partial pressures of the other gas compounds show relatively large variations in terms of concentration (pCH$_4$ from 6.8×10^{-7} to 0.291 bar, pHe from 1×10^{-7} to 1.5×10^{-4} bar, and pH$_2$ from 1.0×10^{-7} to 1.4×10^{-5} bar), with no significant differences among those gases associated with waters having different outlet temperatures (Table 2S).

The δ^{13}C values of dissolved CO$_2$ are calculated from the δ^{13}C-TDIC values using the empirical equation of Zhang et al. (1995), as follows:

$$\delta^{13}C_{CO_2(g)} = \delta^{13}C_{TDIC} - \frac{H_2CO_3}{TDIC}\varepsilon_{(H_2CO_3 - CO_2)} - \frac{HCO_3^-}{TDIC}\varepsilon_{(HCO_3^- - CO_2)}$$
$$- \frac{CO_3^{2-}}{TDIC}\varepsilon_{(CO_3^{2-} - CO_2)}$$

(1)

where the equilibrium molar ratios of aqueous carbon species at sampling temperature and pH, used in Eq. (1), are computed with the PHREEQC code (Parkhurst and Appelo, 2013), whereas the value given by Deuser and Degens (1967) and Mook et al. (1974) is used for the isotope fractionation factor (ε) between dissolved and gaseous CO$_2$. The calculated δ^{13}C-CO$_2$ values range from −27.3 and + 2.94‰ V-PDB (Table 2S).

4.3. Chemical and isotopic composition of free gases

The chemical composition of gases discharged from bubbling pools (Table 1) is dominated by CO$_2$ (from 960 to 994 mmoL/mol), whilst N$_2$ and CH$_4$ concentrations range from 5.1 to 36 and from 0.06 to 2.7 mmoL/mol, respectively. Oxygen and Ar concentrations vary from 0.06 to 2.4 and 0.05–0.76 mmoL/mol, respectively. Hydrogen sulfide is detected in all the gas samples (from 0.02 to 2.1 mmoL/mol), with the only exception of sample 121 (<0.01 mmoL/mol). Hydrogen, He and Ne have concentrations up to
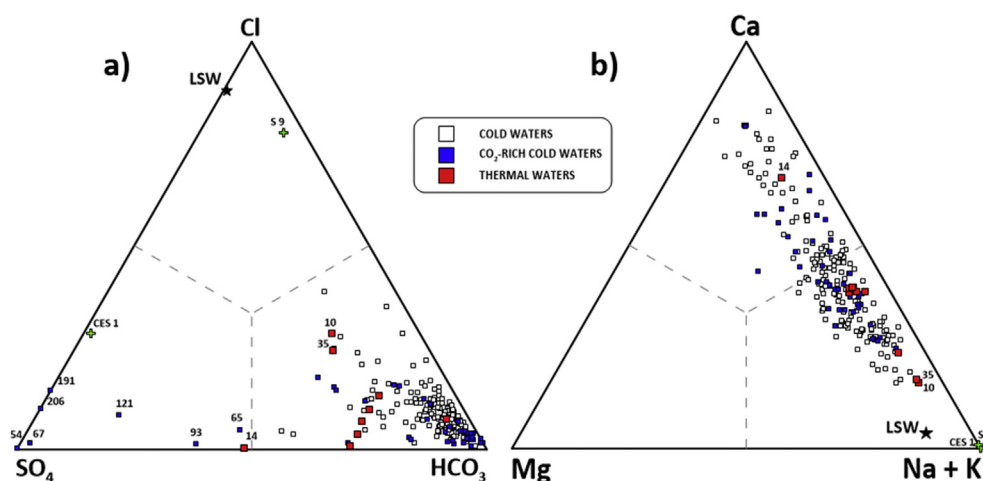

Fig. 2. a) HCO$_3$ − Cl − SO$_4$ and b) (Na + K) − Ca − Mg ternary diagrams for waters from the study area. LSW = local seawater; CES 1, S9 = geothermal wells.

0.05, 0.0045 and 0.0012 mmoL/mol, respectively, while the sum of the C_2-C_4 alkanes range from 0.0002 mmoL/mol (sample 210) to 0.10 mmoL/mol (sample 121). Carbon monoxide is below the analytical detection limit (0.01 mmoL/mol).

The $^{13}C/^{12}C$ isotopic ratios in CO_2 and CH_4 are from −4.7 to +1.0‰ and from −33.4 to −24.9‰ V-PDB, respectively, while the δD-CH_4 values range from −168 to −140‰ V-SMOW. The R/R_a values, corrected for air contamination by using the $^4He/^{20}Ne$ ratios (Poreda and Craig, 1989), vary between 0.07 and 1.04. The $^{40}Ar/^{36}Ar$ ratios of most gases are consistent with that of the atmosphe (295.5; Ozima and Podosek, 2002), whereas samples 50 and 135 show a slight ^{40}Ar-excess (301.4 and 304.9, respectively). The δ^{34}S-H_2S values range from +9.3 to +11.3‰ V-CDT, whereas the δ^{15}N-N_2 values vary from +0.91 to +3.7‰ NBS air.

5. Discussion

5.1. Processes governing the chemical and isotopic composition of waters

As shown in the δD vs. δ^{18}O diagram (Fig. 3a), most cold and thermal waters plot in between the Global Meteoric Water Line (GMWL; Craig, 1961) and the Mediterranean Meteoric Water Line (MMWL; Gat and Carmi, 1970). The only exception is represented by the sample 121, whose strongly negative ^{18}O value is likely resulting by ^{18}O-^{16}O isotopic exchange between H_2O and CO_2 (e.g., Cartwright et al., 2002). The ^{18}O vs. emergence elevation diagram for the cold springs (Fig. 3b) shows a mean isotopic vertical gradient of −0.24‰/100 m, which is similar to those previously calculated for central Italy (Zuppi et al., 1974; Barbieri et al., 2005). This allows to estimate the average altitude of the recharge areas at approximately 300−400 m a.s.l., whereas the generally low vertical drop (~100−200 m) between infiltrating and emergence altitudes suggests that the cold springs pertain to relatively short and shallow hydrological circuits through the volcanic and sedimentary units. Accordingly, the main chemical features of the low-TDS bicarbonate-type cold waters are typical of immature fluids. However, weak water-rock interaction processes occurring in the low-temperature shallow volcanic aquifer favor the mobilization of ions such as K^+ (Fig. 1Sa) and F^- (Fig. 1Sb), whose enrichments in solution are due to their relatively high abundance in the rocks of the Tuscan and Roman volcanic sequences with respect to those occurring in the sedimentary formations (Gambardella et al., 2005; De Rita et al., 2011).

The main chemical features of the *acque acetose*, i.e. high HCO_3^- concentrations and slightly acidic pH (Fig. 4), likely derive from the interaction of the shallow aquifers with the CO_2-rich gas phase released from the deep pressurized regional fluid reservoir (Minissale, 2004). Strongly acidic (pH down to 3.1), SO_4-dominated waters (samples 54, 67, 191, 206; Fig. 4) are produced by near-surface oxidation of H_2S, which is present at significant concentrations in the associated CO_2-rich gas phase, to H_2SO_4 as described by the following chemical reaction (Rye et al., 1992):

$$H_2S + 2O_2 \rightarrow H_2SO_4 \rightarrow 2H^+ + SO_4^{2-} \tag{2}$$
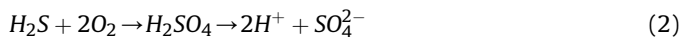
In these waters, O_2 consumption causes reducing conditions and the low pH values, caused by reaction (2), explain the high concentrations of Al, Mn and Fe (Table 1S).

The thermal water discharges are related to the well-recognized regional hydrothermal aquifer hosted in the Mesozoic carbonates at the top of the Triassic anhydrite layers and recharged by meteoric waters from the eastern Apennine range (Chiodini et al., 2000; Minissale, 2004; Minissale and Vaselli, 2011; Cinti et al., 2014). Their main chemical features are indeed dominated by relatively

high concentrations of Ca^{2+}, Mg^{2+}, SO_4^{2-} and HCO_3^-. However, their $[HCO_3^- + SO_4^{2-}]/[Ca^{2+} + Mg^{2+}]$ ratios are >1 (Fig. 5a), i.e. higher than the stoichiometric ratio expected when carbonate and anhydrite dissolution is assumed as the unique source of these ionic species (i.e. $[HCO_3^- + SO_4^{2-}]/[Ca^{2+} + Mg^{2+}] = 1$). This suggests that HCO_3^- and SO_4^{2-} derive, at least partially, from the interaction of waters with the CO_2- and H_2S-rich gases. Few thermal waters (samples 10, 35, 166), i.e. those with the highest TDS values (from 3450 to 4060 mg/L), show relatively high Na^+ and Cl^- concentrations (Table 1S), possibly caused by mixing between the deep thermal fluids uprising from the carbonate-evaporitic aquifer and highly saline waters locally trapped in the Neogene marine sediments below the volcanic sequences (Calamai et al., 1976; Duchi et al., 1992; Dall'Aglio et al., 1994; Minissale et al., 1997b). The possible involvement of the deep and hot Na-Cl brine intercepted from the geothermal wells at Cesano (Calamai et al., 1976) in the chemical features of the Na-Cl-rich thermal waters cannot completely be discarded, since the Na^+/Cl^- molar ratios of these waters are up to 2, i.e. higher than the stoichiometric ratio and approaching that shown by the geothermal fluid (Fig. 5b). However, these relatively high Na^+/Cl^- molar ratios may also be related to Na^+ contribution from alteration processes of silicate minerals (e.g. clay minerals, zeolites or feldspatoids), which are favored by both high temperature and CO_2.

As far as the minor elements are concerned, relatively high Sr concentrations are found in most thermal and SO_4-rich cold waters (Fig. 2Sa), this element being a common Ca^{2+} substituent in carbonate and gypsum/anhydrite minerals, which are abundantly present in the Mesozoic and Triassic reservoir rocks (Barbieri et al., 1979; Minissale et al., 1997b). Lithium and B concentrations, two elements that are typically enriched in geothermal waters, are generally low in both the cold and thermal waters. Exceptions are the above-mentioned Na-Cl-rich thermal waters (samples 10, 35 and 166; Fig. 2Sb,c), whose high concentrations of these elements would support the hypothesis of mixing with saline fluids trapped in the Neogene marine sediments rather than that of fluid contribution from the deep Na-Cl brine. This is confirmed by the very low NH_4^+ concentrations, since this compound typically occurs in the main geothermal reservoirs of Tuscany and Latium (i.e. Larderello, Torre Alfina, Latera, Cesano), deriving from the dissolution of NH_3-rich vapors (Calamai et al., 1976; Duchi et al., 1992; Minissale et al., 1997b).

The degree of maturity of waters from cold and thermal springs interacting with a typical authigenic mineral assemblage (including Na- and K-feldspars, K-micas, chlorite and silica) is commonly investigated on the basis of their Na^+, K^+, and Mg^{2+} concentrations. When water-rock reactions attain a chemical equilibrium, reliable estimations of the fluid reservoir temperatures can be carried out, as described by the following equations (Giggenbach, 1988):

$$T(^\circ C) = 1,390 \Big/ \left(1.75 + log\left[Na^+ \big/ K^+ \right] \right) - 273.15 \tag{3}$$

and

$$T(^\circ C) = 4,410 \Big/ \left(14.0 - log\left[\left(K^+ \right)^2 \big/ Mg^{2+} \right] \right) - 273.15 \tag{4}$$

As shown by the $Na^+/400$-$K^+/10$-$\sqrt{Mg^{2+}}$ ternary diagram (Fig. 3S), the eastern SVD waters are strongly immature, thus the K-Mg and Na-K geothermometers cannot usefully be applied. This is confirmed by the low equilibrium temperatures computed by the silica (chalcedony) geothermometer (Arnorsson et al., 1983) that, according to the concentrations measured in the thermal waters, ranges from 78 to 125 °C, i.e. significantly lower than those measured in the geothermal wells in this area. The unrealistic
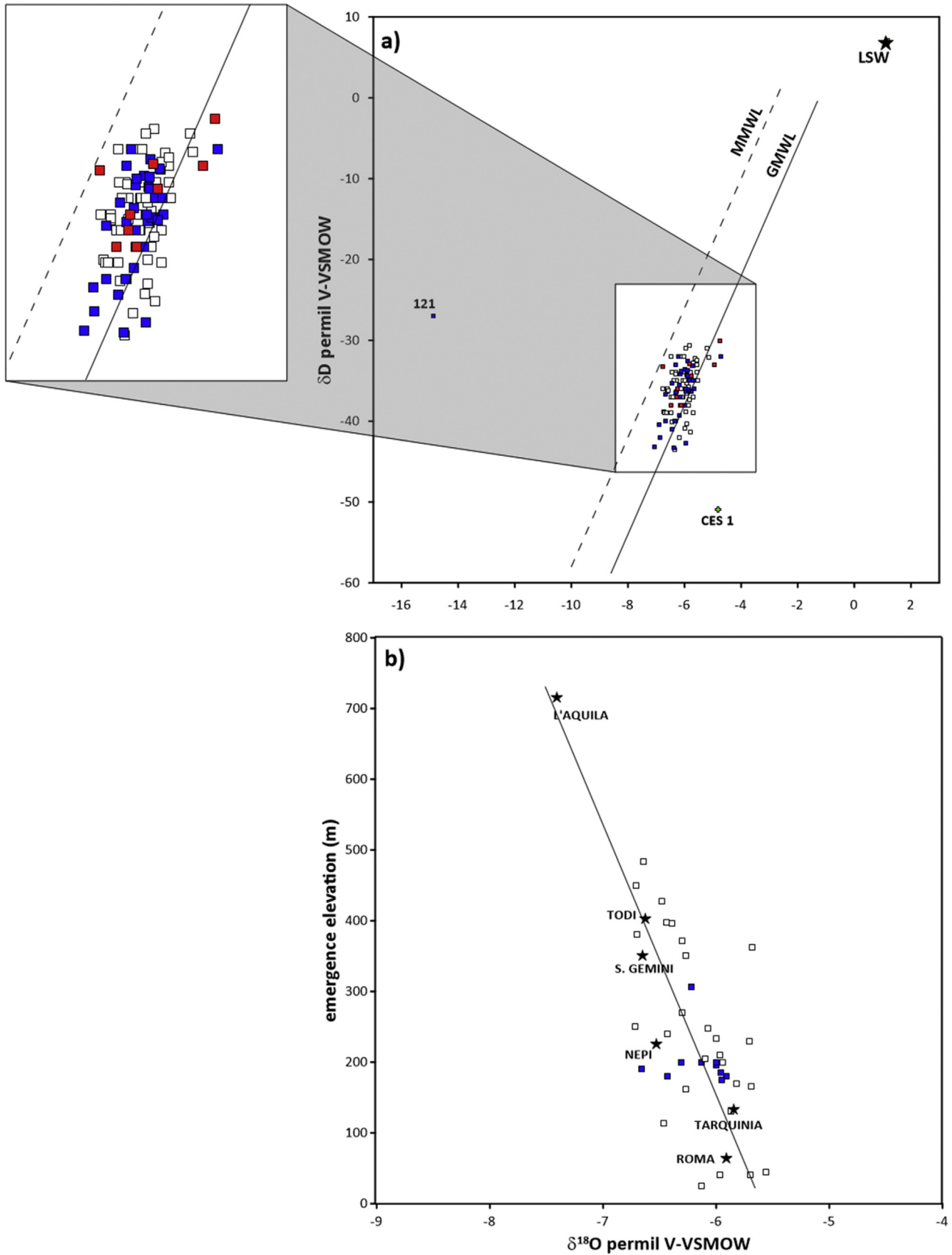
Fig. 3. a) δD vs. δ¹⁸O plot for the collected waters. The solid and the dashed lines delineate the isotopic domain for Global Meteoric Waters (δD = 8δ¹⁸O + 10; Craig, 1961) and that for Mediterranean Meteoric Waters (δD = 8δ¹⁸O + 22; Gat and Carmi, 1970), respectively. LSW = local seawater; b) δ¹⁸O vs. emergence elevation for the collected springs. The dashed line delineates the δ¹⁸O gradient with elevation of 0.24‰/100 m. The δ¹⁸O values of rainwater samples (black stars) from the SVD and surrounding areas are from Longinelli and Selmo (2003). Symbols as in Fig. 2.
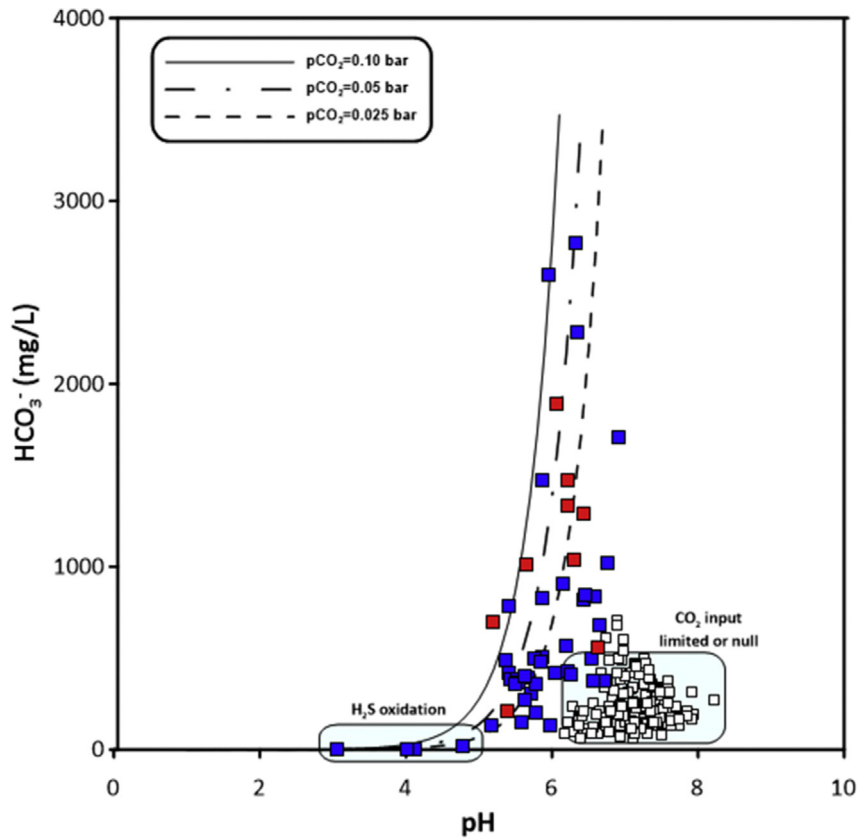
Fig. 4. HCO_3 vs. pH binary diagram for the collected waters. CO_2 saturation curves at pCO_2 = 0.10, 0.05 and 0.025 bar are also reported. Symbols as in Fig. 2.

estimations of fluid temperatures provided by solute geo-thermometers suggest that, even along the main tectonic linea-ments where the fast rising of deep fluids is favored, the chemistry of the thermal fluids is affected by mixing with shallow waters.

5.2. Origin of gas compounds

5.2.1. Carbon species

It is widely accepted (e.g., Minissale et al., 1997b; Chiodini et al., 1999; Minissale, 2004) that the origin of CO_2 in central Italy is related to a twofold source, i.e. mantle degassing ($\delta^{13}C$-CO_2 from −7.0 to −3.0‰ V-PDB; Javoy et al., 1982; Rollinson, 1993) and thermo-metamorphic reactions on carbonates and/or the under-lying metamorphic Palaeozoic basement ($\delta^{13}C$-CO_2 from −2.0 to +2.0‰ V-PDB; Craig, 1963). The $\delta^{13}C$-CO_2 values of the free gases in the eastern SVD, which are in the typical range of gas manifes-tations from the Roman Magmatic Province (Chiodini et al., 2000, 2007; Minissale, 2004; Cinti et al., 2011, 2014), are consistent with this hypothesis. The relatively high $CO_2/^3He$ values (up to 6.0×10^{12}; Fig. 6a), i.e. exceeding more than three orders of magnitude that of MORB mantle (1.4×10^9; Marty and Jambon, 1987), support a dominant CO_2 crustal source. According to the correlation between the calculated $\delta^{13}C$ values of dissolved CO_2 and the pCO_2 values (Fig. 6b), CO_2 in the CO_2-poor cold waters likely originates from soil respiration (e.g., Cerling et al., 1991; Cartwright et al., 2002), whereas the isotopically heavy CO_2 from the CO_2-rich cold and thermal waters has the same deep crustal/mantle source feeding the bubbling gases. Dissolved CO_2 in waters showing in-termediate pCO_2 values is likely due to mixing processes between these two end-members.

Methane is defined as microbial (or biogenic), when produced

by (i) metabolic processes of microbial communities at relatively low temperatures (<120 °C; Takai et al., 2008) or (ii) thermal degradation of organic matter at higher (>150 °C) temperatures (Quigley and Mackenzie, 1988; Tang et al., 2000; Mango, 2001). The most widely accepted geochemical tool to determine the dominant sources of CH_4 is based on both the composition of its stable iso-topes ($^{13}C/^{12}C$ and $^2H/^1H$) (Schoell, 1980) and the $CH_4/(C_2H_6+C_3H_8)$ ratios (Bernard et al., 1978; Whiticar et al., 1986; Whiticar, 1999). Tassi et al. (2012) recently revisited this classical approach. These authors argued that CH_4 production of most CO_2-dominated gas discharges in peri-Tyrrhenian central Italy, including those from western SVD (Cinti et al., 2011), was related to CO_2 reduction. This hypothesis was based on the observation that both the $CH_4/(C_2H_6+C_3H_8)$ ratios and $\delta^{13}C$-CH_4 values were much higher than those expected for a typical thermogenic CH_4. Noteworthy, this CH_4 genetic process cannot be recognized for the gas emissions from eastern SVD, since their $\delta^{13}C$-CH_4, δD-CH_4, and $CH_4/(C_2H_6+C_3H_8)$ values are consistent with a prevailing thermogenic source (Fig. 7a and b).

5.2.2. Inert gas species

Helium, Ar and N_2 can be used as geochemical tracers to recognize primary fluid sources since they are chemically inert. As shown by the He-N_2-Ar diagram (Fig. 8; Giggenbach, 1992), most gases from the eastern SVD plot close to the air or air-saturated water (ASW) composition, indicating relatively small extra-atmospheric contribution for both He and N_2. The latter, possibly related to reactions involving metasedimentary rocks (Honma and Itihara, 1981; Mingram and Brauer, 2001), is also suggested by the positive $\delta^{15}N$-N_2 values (up to +3.7‰ NBS air). On the contrary, the occurrence of dominant air-derived Ar is supported by the

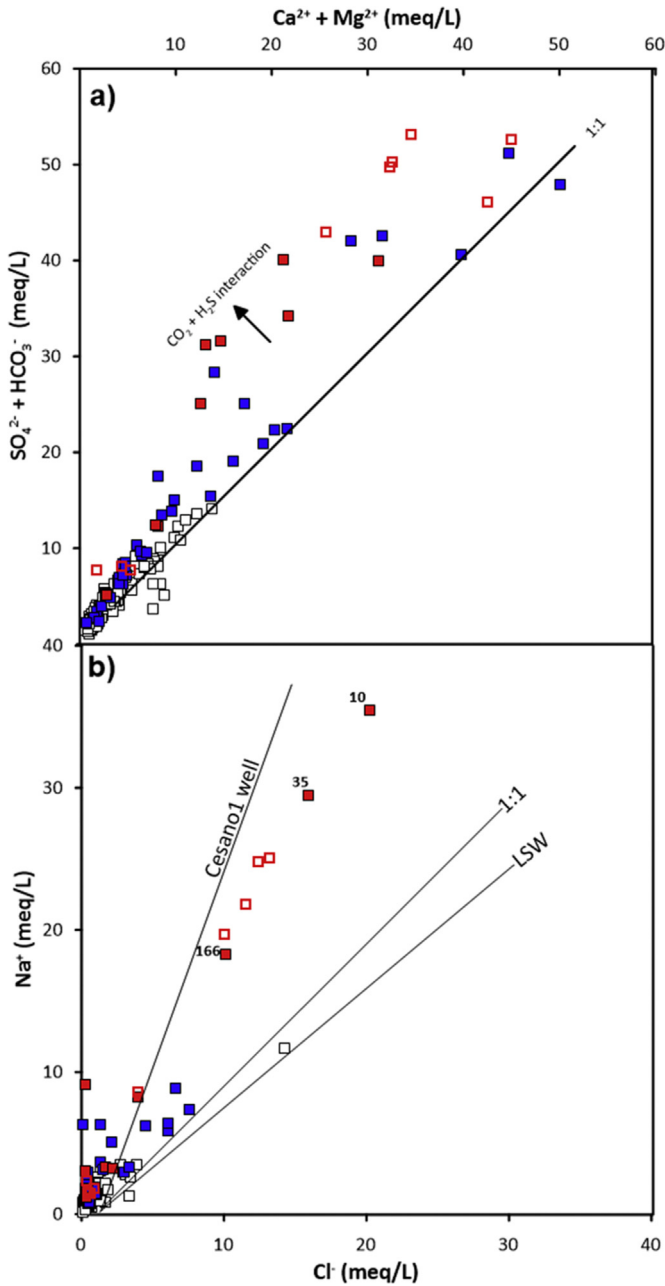Fig. 5. a) $Ca^{2+} + Mg^{2+}$ vs. SO_4^{2-}/HCO_3^- and b) Na vs. Cl^- correlation plots for the collected waters. Samples of Stigliano (red open squares) are from Cinti et al. (2011). Symbols as in Fig. 2. (For interpretation of the references to colour in this figure legend, the reader is referred to the web version of this article.)

Fig. 6. a) $CO_2/^3He$ vs. $\delta^{13}C$-CO_2 correlation plot for free gases. Boxes and mixing curves between the three end-members are from Sano and Marty (1995). Data for the western SVD gases are from Cinti et al. (2011); b) $\delta^{13}C$-CO_2 in equilibrium with water vs. pCO_2 (bar). Symbols as in Fig. 2.

relatively low $^{40}Ar/^{36}Ar$ ratios (<305), i.e. close to atmospheric ratio (295.5; Marty, 1995). As far as the origin of He is concerned, the $^3He/^4He$ ratios can discriminate (i) ^{4}He-rich gases from radioactive decay processes, mostly occurring in the crust and typically producing R/Ra values from 0.01 to 0.1 (O'Nions and Oxburgh, 1988), and (ii) ^{3}He-rich gases related to a mantle source (Polyak and Tolstikhin, 1985). A pronounced northward decrease of the R/Ra values in gas emissions (Hooker et al., 1985; Minissale, 2004) and fluid inclusions in olivine and clinopyroxene phenocrysts from the Quaternary rocks (Martelli et al., 2004) was observed from southern Italy (Mt. Etna and the Aeolian Islands) up to the Roman Magmatic Province. This feature was ascribed to mantle contamination via subduction of the Ionian-Adriatic plate beneath central-
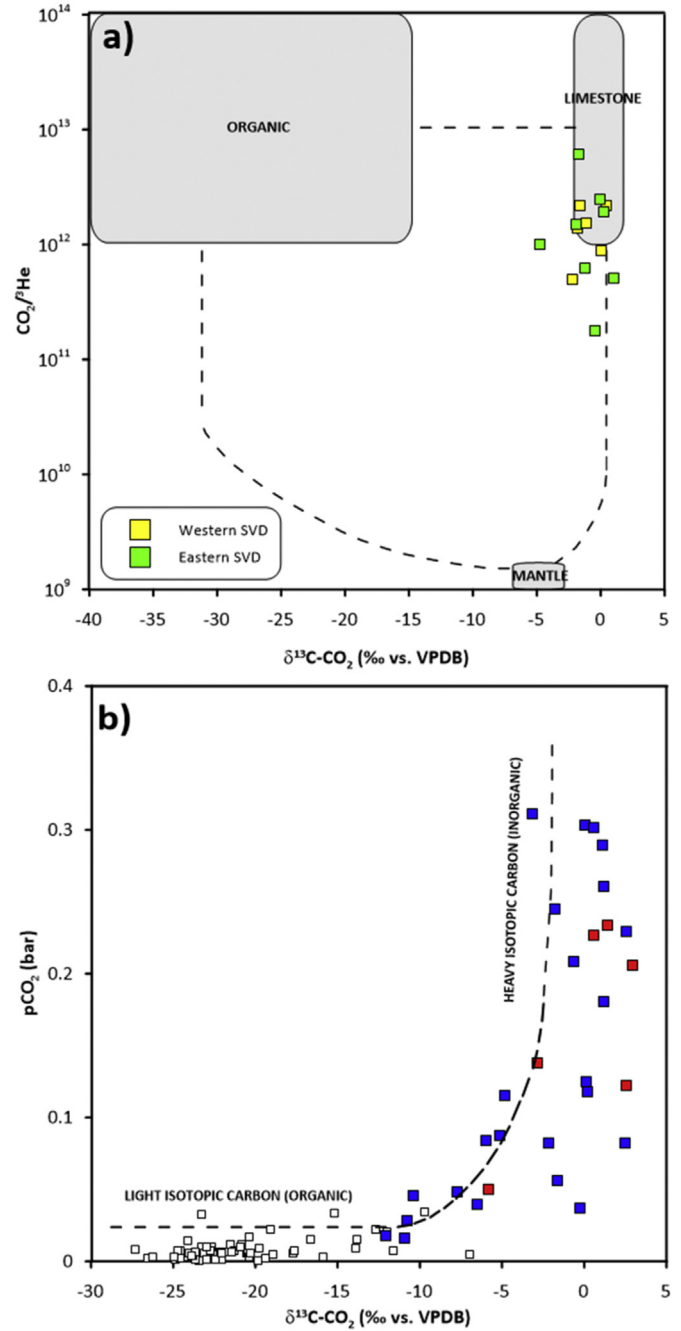
southern Italy (Peccerillo, 1999; Martelli et al., 2004, 2008). The R/Ra ratios from the eastern SVD (from 0.07 to 1.04) are consistent with this general hypothesis, since they range within the values measured in gas emissions from the Roman Magmatic Province (Minissale, 2004; Barberi et al., 2007; Chiodini et al., 2007; Cinti et al., 2011) and are significantly lower than those found in the active volcanoes of southern Italy, e.g., 2.0—3.2 at Campi Flegrei, (Tedesco et al., 1990), 2.2—2.7 at Mt. Vesuvius (Federico et al., 2002), 6.5—6.9 at Mt. Etna (Allard et al., 1997; Tedesco, 1997). The eastern SVD isotopic values reflect a prevailing crustal-radiogenic source with a minor amount of mantle He. Assuming R/Ra ~6.5 as the
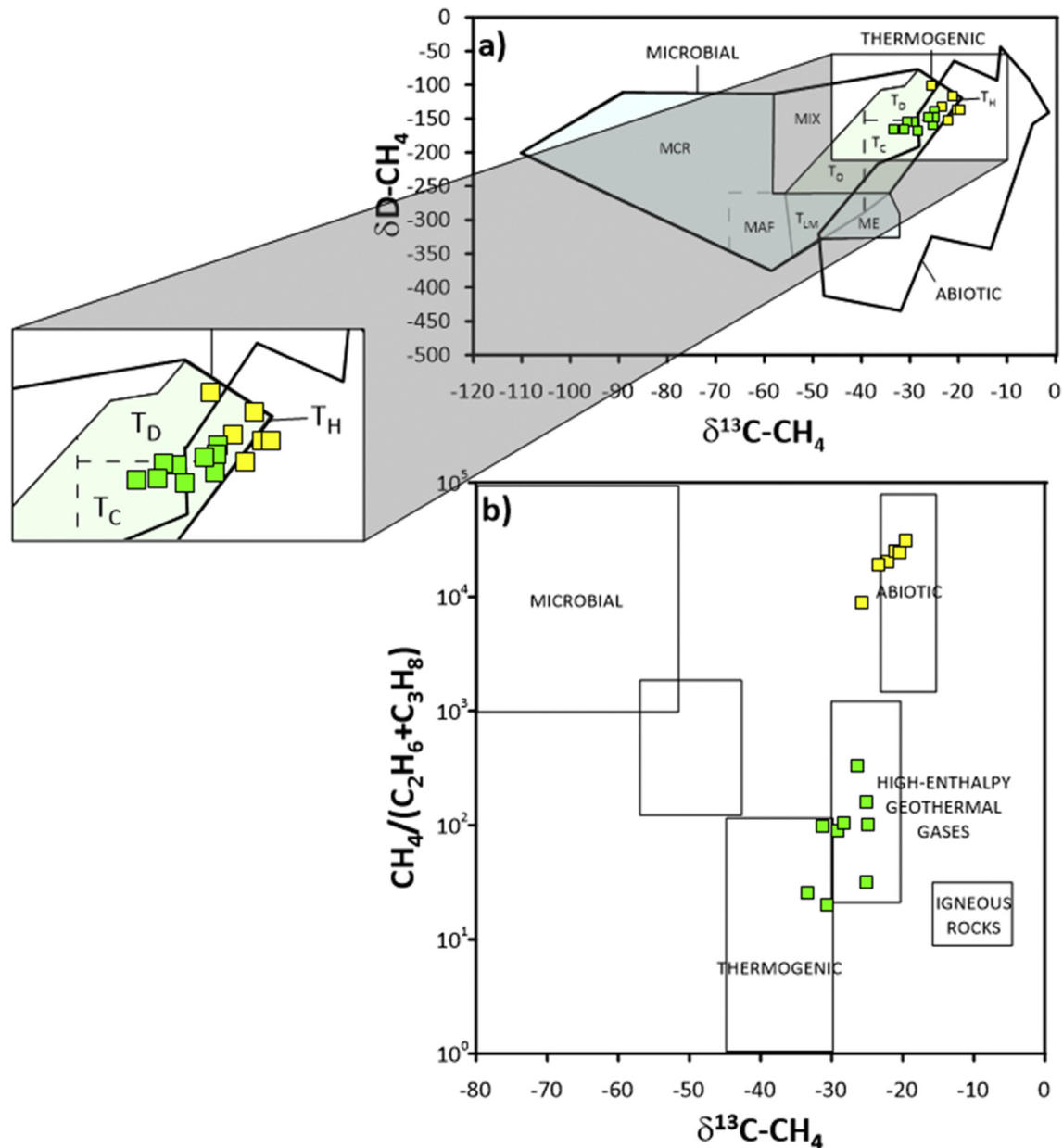
Fig. 7. (a) $\delta^{13}C$-CH_4 vs. δD-CH_4 diagram for free gases. Fields and boxes are from Etiope (2015). MRC = microbial carbonate reduction, MAF = microbial acetate fermentation, ME = microbial in evaporitic environment, T_O = thermogenic with oil, T_C = thermogenic with condensate, T_D = dry thermogenic, T_H = thermogenic with high-temperature CO_2-CH_4 equilibration, T_{LM} = thermogenic low maturity; (b) $CH_4/(C_2H_6+C_3H_8)$ vs. $\delta^{13}C$-CH_4 diagrams for free gases. Fields and boxes are from McCollom and Seewald (2007). Data for the western SVD gases are from Cinti et al. (2011). Symbols as in Fig. 6a.

mantle end-member in central-southern Italy (Tedesco, 1997), i.e. similar to the European sub-continental mantle (Dunai and Baur, 1995), the mantle He fraction in the study area is estimated at 0.8—16%.

5.2.3. Reduced inorganic gases (H_2S and H_2)

Hydrogen sulfide in volcanic gas discharges is mainly produced by disproportionation of SO_2 (Giggenbach, 1987; Allard et al., 1991; Oppenheimer et al., 2014), whereas sedimentary sources of H_2S consist of: 1) alteration of sulfide minerals (e.g. pyrite; Giggenbach, 1980; Chiodini, 1994), 2) microbial activity (Thode, 1991) and 3) thermo-chemical sulfate reduction (Machel et al., 1995; Worden and Smalley, 1996). Hydrothermal gases are characterized by the virtual absence of SO_2 and the presence of H_2S as unique S-bearing gaseous species (Giggenbach, 1980), whose origin can usefully be

investigated by using the $\delta^{34}S$-H_2S values (e.g., Ault and Kulp, 1959; Sakai, 1968; Marini et al., 2011). The strongly positive $\delta^{34}S$-H_2S values of the eastern SVD gases (from 9.5 to 10.6‰ V-CDT) suggest to discard a H_2S volcanic source, since the $\delta^{34}S$ of magma-derived sulfur in volcanic rocks and gases is ~0‰ V-CDT (Allard et al., 1991; de Moor et al., 2013). It is worth mentioning that the $\delta^{34}S$ values of sulfide deposits in the SVD are mainly negative (averaging −2.6‰ V-CDT; Cavarretta and Lombardi, 1992), whereas evaporitic sulfates from Triassic anhydrites (Burano Fm.) have $\delta^{34}S$ values ranging from 13.6 to 17.4‰ V-CDT (Cortecci et al., 1981), and the $\delta^{34}S$-SO_4^{2-} values in Ca-SO_4 thermal waters are typically ~+14‰ V-CDT (Zuppi et al., 1974; Cavarretta and Lombardi, 1992; Cinti et al., 2014). Hence, H_2S in the eastern SVD gases likely derives from thermo-chemical reduction of anhydrites, according to re-actions involving CO_2 and CH_4, as follows (Giggenbach, 1980;
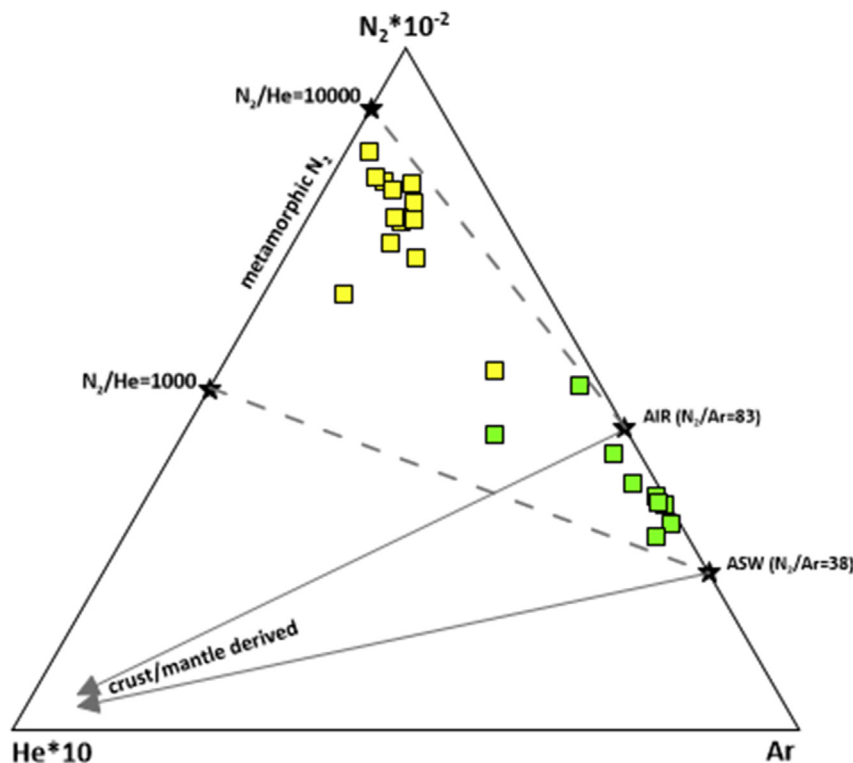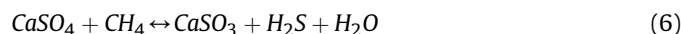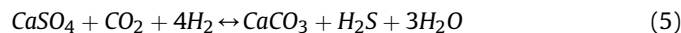
Fig. 8. Ar-N$_2$-He ternary diagram (Giggenbach, 1992) for free gases. The proportions among the three gases were calculated by using the concentrations in μmol/mol. ASW = air saturated water at 20 °C. Data for the western SVD gases are from Cinti et al. (2011). Symbols as in Fig. 6a.

Worden and Smalley, 1996):

$$CaSO_4 + CO_2 + 4H_2 \leftrightarrow CaCO_3 + H_2S + 3H_2O \qquad (5)$$

$$CaSO_4 + CH_4 \leftrightarrow CaSO_3 + H_2S + H_2O \qquad (6)$$

It is worth noting that the δ^{34}S-H$_2$S values isotopic values of the SVD gases are slightly lower than those of the evaporitic sulfates (2–6‰). This implies that the isotopic fractionation affecting S during the reactions (5) and (6) occurs at relatively high temperatures (≥200 °C) (Ohmoto and Rye, 1979; Machel et al., 1995). Accordingly, the source region of H$_2$S in the study area corresponds to the main hydrothermal reservoir where temperatures of ~300 °C were measured (Allegrini et al., 1982). By assuming this hypothesis as valid, CH$_4$ and H$_2$ likely originate within the same deep fluid reservoir, being involved in the reactions (5) and (6).

5.2.4. Gas geothermometry

The temperatures of a hydrothermal fluid reservoir can be estimated by applying a variety of geothermometers based on the chemical composition of gas discharges (e.g. Giggenbach, 1987; Chiodini and Marini, 1998). Since the eastern SVD gases are associated with bubbling pools, the concentrations of water vapor and CO mostly depend on interaction with liquid water at the surface, and therefore only low soluble gas compounds, such as CH$_4$, CO$_2$ and H$_2$, can be used for geothermometric applications. Gas equilibria in the CH$_4$-CO$_2$-H$_2$ system are controlled by the following reaction (Giggenbach, 1987, 1996):

$$CH_4 + 2H_2O \leftrightarrow CO_2 + 4H_2 \qquad (7)$$
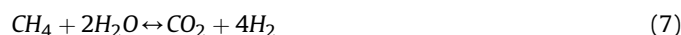
As shown in the log (XH$_2$/XAr*) vs. log (XCH$_4$/XCO$_2$) binary diagram (Fig. 9), where the Ar* values (Ar* = Ar-O$_2$/22, since the O$_2$/Ar ratio in air is 22) is used to minimize the effect of air contamination occurring at the surface, the eastern SVD gases plot along the

equilibrium curve of a liquid phase at redox conditions fixed by the D'Amore and Panichi (1980) buffer. Under these redox conditions, which are typical for hydrothermal fluids, the estimated temperatures of the eastern SVD gases range from 100 to 200 °C, i.e. values considerably lower than those measured in the geothermal wells (~300 °C). The most reliable explanation is that re-equilibrium processes at lower temperatures affect H$_2$ and CH$_4$ during the up-rising of fluids from the hydrothermal reservoir. However, the wide variations (~2 log-units) of both the XH$_2$/XAr* and the XCH$_4$/XCO$_2$ ratios suggest that the concentrations of these gases are mostly depending on other processes than reaction (7). For example, the CH$_4$/(C$_2$H$_6$+C$_3$H$_8$) ratios and δ^{13}C-CH$_4$, and δD-CH$_4$ values indicate that CH$_4$ is dominantly produced by thermal degradation of organic matter, thus the behavior of this organic gas cannot be considered exclusively controlled by CO$_2$ reduction.

A further exercise to provide insights into the fluid temperatures at depth can be carried out considering the H$_2$S-H$_2$-H$_2$O system, as described by the following reaction (Chiodini et al., 2001):

$$FeS_2 + H_2O_{(vap)} + [H_2O] \leftrightarrow [FeO] + \frac{1}{2}O_2 + 2H_2S \qquad (8)$$
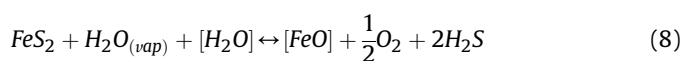
where [FeO] is an unspecified Fe-Al silicate and [H$_2$O] the corresponding Al-silicate in its protonated, Fe-free, form. As already mentioned, the concentration of water vapor in the gases from the bubbling pools is controlled the condensation at the surface, thus calculations of gas equilibria in the H$_2$S-H$_2$-H$_2$O system are carried out using the H$_2$O$_{vap}$ concentrations computed on the basis of the gas-water ratio (X$_g$) that is estimated, as follows (Taran, 2005):

$$X_g = \frac{0.0015}{Ar} - 0.0011P_t \qquad (9)$$

where P$_t$, i.e. the air pressure at the recharge altitude, is

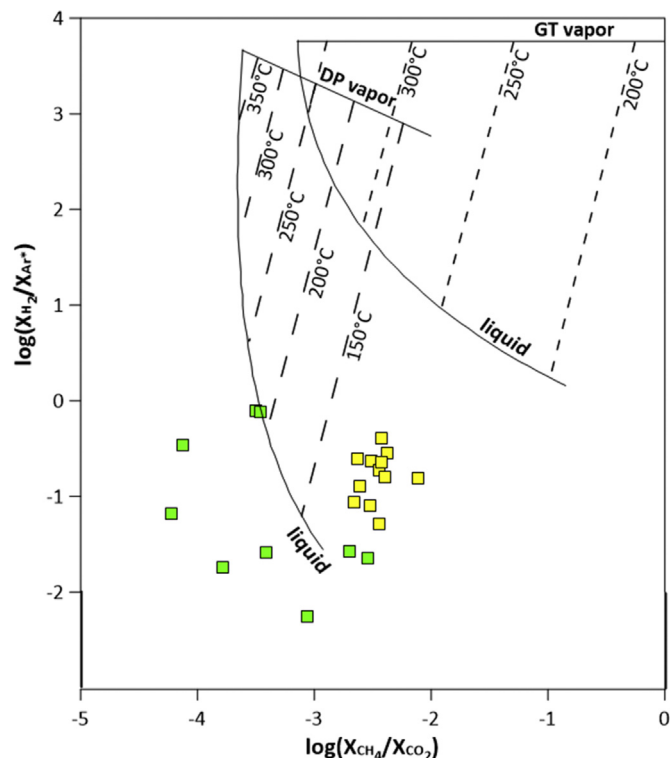**Fig. 9.** Plot of log (X_{CH4}/X_{CO2}) vs. log (X_{H2}/X_{Ar^*}). The theoretical grids assume that redox conditions in the gas equilibration zone are controlled by the FeO-FeO$_{1.5}$ hydrothermal buffer (Giggenbach, 1987) and the DP buffer (D'Amore and Panichi, 1980). Data for the western SVD gases are from Cinti et al. (2011). Symbols as in Fig. 6a.

0.878 atm at 10 °C and 1000 m a.s.l., and Ar is assumed as entirely atmospheric. The relatively large variation of the X_{H2S}/X_{H2O} ratios (~2 log-units) in the log (X_{H2S}/X_{H2O}) vs. log (X_{H2}/X_{H2O}) binary diagram (Fig. 4S) coupled with the significantly lower equilibrium temperatures with respect to those measured in geothermal wells, confirms that secondary processes, i.e. loss of H_2S due to its relatively high solubility and oxidation in the liquid phase, likely affect the deep gases during their ascent.

6. Eastern vs. western SVD

Although fluid discharges from the eastern and the western sectors of SVD are considered to pertain to a unique hydrothermal system (Fig. 10), the chemical and isotopic compositions of waters and gases from the two sectors show some significant differences.

Thermal waters showing relatively high Na^+ and Cl^- concentrations occur in both the eastern and the western SVD, although

only in the western sector (i.e. at Stigliano; Cinti et al., 2011) they are associated with high NH_4/Cl, B/Cl and Li/Cl ratios and to a marked ^{18}O enrichment, as related to fluids contribution from a deep geothermal brine. Moving eastward, the significantly lower NH_4^+ concentrations and B/Cl and Li/Cl ratios (Fig. 2Sb,c) and the meteoric signature of the Na-Cl-rich thermal waters, suggest that the most reliable source of these compounds likely consist of highly saline waters locally trapped in the Neogene marine sediments. Some contribution from a deep Na-Cl geothermal brine, as that intercepted by geothermal wells at Cesano, seems unlike, although it cannot completely be ruled out.

With respect to the gas emissions, those discharging from the eastern SVD, showing relatively high N_2 and Ar concentrations (Table 1), and low N_2/Ar (Fig. 8) and $\delta^{15}N$-N_2 values (Table 1), are marked by a higher contribution from air with respect to the western SVD gases. Accordingly, equilibrium temperature estimations computed according to both the CH_4-CO_2-H_2 and the H_2S-H_2-H_2O geothermometers for the eastern SVD gases are not reliable since they show too large variations. On the contrary, computed temperatures by using the same theoretical approach for the gases from the western SVD sector (Cinti et al., 2011) cluster around at ~175 °C, although significantly lower than those measured at depth. A further important distinction in the fluid chemistry of the two areas is highlighted by the C_1/C_{2+} ratios and $\delta^{13}C$-CH_4 and δD-CH_4 values (Fig. 7): the eastern SVD gases show the typical features of thermogenic CH_4, whereas CO_2 reduction is the main production mechanism of CH_4 in the gas emissions from western SVD (Cinti et al., 2011).

Summarizing, fluids from the western and the eastern sectors of SVD show some significant differences, mainly due to a higher contribution of shallow secondary processes in the eastern SVD, which are able to significantly mask the chemistry of the uprising deep fluids. One possible explanation for this spatial compositional distribution is that the cooling and diluting effects of meteoric water from the Apennine chain are particularly efficient in the easternmost fluid discharges, since they are closer to this important recharge area with respect to those emerging in the westernmost ones. The enhanced contribution of meteoric water to the uprising hydrothermal fluids also produces the relatively high air contamination characterizing the eastern SVD gases.

7. Conclusions

The SVD hosts a water-dominated hydrothermal reservoir at T~300 °C that discharges Ca-HCO$_3$(SO$_4$) to Na(Ca)-HCO$_3$(Cl) waters, mostly emerging along the borders of buried horst-graben structures, where extensional fractures and faults provide permeable pathways for their ascent to the surface (Fig. 10). A CO_2(H_2S)-rich gas phase is occasionally associated with the thermal fluid discharges, although the frequent occurrence of CO_2-rich cold waters
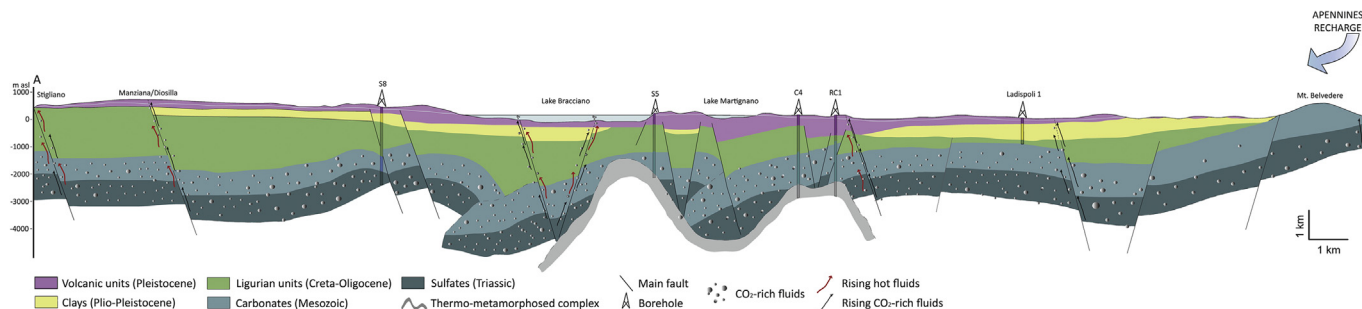

Fig. 10. Interpretative conceptual model of groundwater circulation in the Sabatini Volcanic District.

(*acque acetose*) indicates that a significant amount of deep-originated gases is discharged through diffuse soil degassing. The isotopic signature of CO_2 and He suggests that these gases mainly have a crustal origin with minor contribution from mantle degassing. Cold Ca(Na)-HCO$_3$ waters are not affected by the hydrothermal system, being located far from the main tectonic alignments. Hence, in the absence of tectonic disturbance, the shallow volcanic and sedimentary formations efficiently isolate the hydrothermal reservoir from the surface. Meteoric waters from local highs and the Apennine range recharge both the shallow and deep reservoirs. By comparing the hydrothermal fluids discharging in the western and eastern sector of SVD, the latter are strongly influenced at relatively shallow depth by the cold and air-rich meteoric water recharge from the Apennine range. No clear clues of the Na-Cl brine discharged from the Cesano geothermal wells are recognized at the surface, even where the tectonic setting locally favors the uprising of the hydrothermal fluids. Although masked by mixing processes with the shallow aquifer, the deep hydrothermal reservoir of eastern SVD is to be considered an important potential resource, especially considering the recent renewed interest for geothermal energy in Italy. In the past the exploitation through conventional technologies was strongly limited by the fluid characteristics (i.e. high salinity of the liquid phase and presence of corrosive gases). Presently, the most recent unconventional technologies can make possible the exploitation of the geothermal resources through binary systems where a working fluid, generally constituted by organic compounds (propane), is used in place of the geothermal fluid to produce electricity (Di Pippo, 2008). Moreover, direct uses (e.g. building heating and cooling, fish farming, greenhouse heating), which imply relatively low costs, may represent, at a local scale, more than a valid alternative for the exploitation of these thermal fluids.

Acknowledgements

Appendix A. Supplementary data

Supplementary data related to this article can be found at http://dx.doi.org/10.1016/j.apgeochem.2017.06.014.

References

Acocella, V., Funiciello, R., 2006. Transverse systems along the extensional Tyrrhenian margin of central Italy and their influence on volcanism. Tectonics 25. http://dx.doi.org/10.1029/2005TC001845.

Allard, P., Maiorani, A., Tedesco, D., Cortecci, G., Turi, B., 1991. Isotopic study of the origin of sulfur and carbon in Solfatara fumaroles, Campi Flegrei caldera. J. Volcanol. Geotherm. Res. 48, 139–159.

Allard, P., Jean-Baptiste, P., D'Alessandro, W., Parello, F., Parisi, B., Flehoc, C., 1997. Mantle derived helium and carbon in groundwater and gases of Mount Etna. Italy. Earth Planet. Sci. Lett. 148, 501–516.

Allegrini, G., Corsi, R., Culivicchi, G., Di Falco, R., Fiordelisi, A., Grassi, A., Nardini, G., Nencetti, G.F., Tomei, B., 1982. Fluid management of the Cesano reservoir: experimental activity. In: proceedings of the 1st Turkish-Italian seminar on geothermal energy, Ankara and Kizildere, Turkey, Sept. 6-28, 1982. Comp. Exam. Kizildere Cesano Geotherm. Fields II, 143–206.

Arnorsson, S., Gunnlaugsson, E., Svavarsson, H., 1983. The chemistry of geothermal waters in Iceland − II. Mineral equilibria and independent variables controlling water compositions. Geochim. Cosmochim. Acta 47, 547–566.

Ault, W.U., Kulp, J.L., 1959. Isotopic geochemistry of sulphur. Geochim. Cosmochim. Acta 16, 201–235.

Baldi, P., Ferrara, G.C., Masselli, L., Pieretti, G., 1973. Hydrogeochemistry of the region between monte amiata and Rome. Geothermics 2, 124–141.

Barberi, F., Buonasorte, G., Cioni, R., Fiordalisi, A., Foresi, L., Iaccarino, S., Laurenzi, M.A., Sbrana, A., Vernia, L., Villa, I.M., 1994. Plio-Pleistocene geological evolution of the geothermal area of Tuscany and Latium. Mem. Descr. della Carta Geol. d'Italia 49, 77–134.

Barberi, F., Carapezza, M.L., Ranaldi, M., Tarchini, L., 2007. Gas blowout from shallow boreholes at Fiumicino (Rome): induced hazard and evidence of deep CO_2 degassing on the Tyrrhenian margin of central Italy. J. Volcanol. Geotherm. Res. 165, 17–31.

Barbieri, M., Boschetti, T., Petitta, M., Tallini, M., 2005. Stable isotope (²H, ¹⁸O and ⁸⁷Sr/⁸⁶Sr) and hydrochemistry monitoring for groundwater hydrodynamics analysis in a karst aquifer (Gran Sasso, central Italy). Appl. Geochem 20, 2063–2081.

Barbieri, M., Masi, U., Tolomeo, L., 1979. Origin and distribution of strontium in the travertines of Latium (central Italy). Chem. Geol. 24, 181–188.

Bernard, B.B., Brooks, J.M., Sackett, W.M., 1978. A Geochemical Model for Characterization of Hydrocarbon Gas Sources in Marine Sediments. Proc. of the Offshore Technology Conference, Houston, USA, pp. 435–438.

Billi, B., Cappetti, G., Luccioli, F., 1986. ENEL activity in the research, exploration and exploitation of geothermal energy in Italy. Geothermics 15, 765–779.

Buonasorte, G., Carboni, M.G., Conti, M.A., 1991. Il substrato plio-pleistocenico delle vulcaniti sabatine: considerazioni stratigrafiche e paleoambientali. Boll. Soc. Geol. It 110, 35–40.

Buonasorte, G., Cameli, G.M., Fiordalisi, A., Parotto, M., Perticone, I., 1995. Results of Geothermal Exploration in Central Italy (Latium-campania). Proc. of the World Geothermal Congress, Florence, Italy, pp. 1293–1298.

Calamai, A., Cataldi, R., Dall'Aglio, M., Ferrara, G., 1976. Preliminary report on the Cesano hot brine deposit (Northern Latium, Italy). Proc. U.N. Symp. Development Use Geotherm. Energy, S. Francisco, USA 305–313.

Capasso, G., Inguaggiato, S., 1998. A simple method for the determination of dissolved gases in natural waters. Appl. Therm. waters Vulcano Isl. Appl. Geochem 13, 631–642.

Capelli, G., Mazza, R., Gazzetti, C., 2005. In: Pitagora (Ed.), Strumenti e strategie per la tutela e l'uso compatibile della risorsa idrica nel Lazio: gli acquiferi vulcanici, p. 191.

Cartwright, I., Weaver, T., Tweed, S., Ahearne, D., Cooper, M., Czapnik, K., Tranter, J., 2002. Stable isotope geochemistry of cold CO_2-bearing mineral spring waters, Daylesford, Victoria, Australia: sources of gas and water and links with waning volcanism. Chem. Geol. 185, 71–91.

Cavarretta, G., Lombardi, G., 1992. Origin of sulphur in minerals and fluids from Latium (Italy): isotopic constraints. Eur. J. Mineral. 4, 1311–1329.

Cavarretta, G., Tecce, F., 1987. Contact metasomatic and hydrothermal minerals in the SH2 well, Sabatini volcanic district, Latium, Italy. Geothermics 2, 127–145.

Cerling, T.E., Solomon, D.K., Quade, J., Bowman, J.R., 1991. On the isotopic composition of carbon in soil carbon dioxide. Geochim. Cosmochim. Acta 55, 3403–3405.

Chiodini, G., 1994. Temperature, pressure and redox conditions governing the composition of the cold CO_2 gases discharged in north Latium (central Italy). Appl. Geochem 9, 287–295.

Chiodini, G., Baldini, A., Barberi, F., Carapezza, M.L., Cardellini, C., Frondini, F., Granieri, D., Ranaldi, M., 2007. Carbon dioxide degassing at Latera caldera (Italy): evidence of geothermal reservoir and evaluation of its potential energy. J. Geophys. Res. 112 http://dx.doi.org/10.1029/2006JB004896.

Chiodini, G., Frondini, F., Cardellini, C., Parello, F., Peruzzi, L., 2000. Rate of diffuse carbon Earth degassing estimated from carbon balance of regional aquifers: the case of central Apennine. Italy. J. Geophys. Res. 105, 8423–8434.

Chiodini, G., Frondini, F., Kerrick, D.M., Rogie, J., Parello, F., Peruzzi, L., Zanzari, A.R., 1999. Quantification of deep CO_2 fluxes from central Italy. Examples of carbon balance for regional aquifers and of soil diffuse degassing. Chem. Geol. 159, 205–222.

Chiodini, G., Marini, L., 1998. Hydrothermal gas equilibria: the H_2O-H_2-CO_2-CO-CH_4 system. Geochim. Cosmochim. Acta 62, 2673–2687.

Chiodini, G., Marini, L., Russo, M., 2001. Geochemical evidence for the existence of high-temperature hydrothermal brines at Vesuvio volcano, Italy. Geochim. Cosmochim. Acta 65, 2129–2147.

Cimarelli, C., De Rita, D., 2006. Relatively rapid emplacement of dome-forming magma inferred from strain analyses: the case of the acid dome complexes (central Italy). J. Volcanol. Geotherm. Res. 158, 106–116.

Cinti, D., Procesi, M., Tassi, F., Montegrossi, G., Sciarra, A., Vaselli, O., Quattrocchi, F., 2011. Fluid geochemistry and geothermometry in the western sector of the Sabatini volcanic district and the Tolfa Mountains (Central Italy). Chem. Geol. 284, 160–181.

Cinti, D., Tassi, F., Procesi, M., Bonini, M., Capecchiacci, F., Voltattorni, N., Vaselli, O., Quattrocchi, F., 2014. Fluid geochemistry and geothermometry in the unexploited geothermal field of the Vicano-Cimino Volcanic District (Central Italy). Chem. Geol. 371, 96–114.

Cioni, R., Laurenzi, M.A., Sbrana, A., Villa, I.M., 1993. ⁴⁰Ar-³⁹Ar chronostratigraphy of the initial activity in the Sabatini Volcanic Complex (Italy). Boll. Soc. Geol. It 112, 251–263.

Cortecci, G., Reyes, E., Berti, G., Casati, P., 1981. Sulfur and oxygen isotopes in Italian marine sulfate of Permian and Triassic age. Chem. Geol. 34, 65–79.

Craig, H., 1961. Isotopic variations in meteoric waters. Science 133, 1702–1703.

Craig, H., 1963. The isotopic geochemistry of water and carbon in geothermal areas. In: Tongiorgi, E. (Ed.), Nuclear Geology on Geothermal Areas. CNR (Italian

Council for Research), Spoleto, Italy, pp. 17–54.

Dall'Aglio, M., Duchi, V., Minissale, A., Guerrini, A., Tremori, M., 1994. Hydrogeochemistry of the volcanic district in the Tolfa and Sabatini Mountains in central Italy. J. Hydrol. 154, 195–217.

D'Amore, F., Panichi, C., 1980. Evaluation of deep temperature of hydrothermal systems by a new gas-geothermometer. Geochim. Cosmochim. Acta 44, 549–556.

Della Vedova, B., Pellis, G., Foucher, J.P., Rehault, J.P., 1984. Geothermal structure of Tyrrhenian sea. Mar. Geol. 55, 271–289.

de Moor, J.M., Fischer, T.P., Sharp, Z.D., King, P.L., Wilke, M., Botcharnikov, R.E., Cottrell, E., Zelenski, M., Marty, B., Klimm, K., Rivard, C., Ayalew, D., Ramirez, C., Kelly, K.A., 2013. Sulfur degassing at Erta Ale (Ethiopia) and Masaya (Nicaragua) volcanoes: implications for degassing processes and oxygen fugacities of basaltic systems. Geochem. Geophys. Geosyst. http://dx.doi.org/10.1022/ggge.20255.

De Rita, D., Di Filippo, M., Rosa, C., 1996. Structural evolution of the Bracciano volcano-tectonic depression, Sabatini volcanic district, Italy. In: McGuire, W.C., et al. (Eds.), Volcano Instability on the Earth and Other Planets, vol. 110. Geol. Soc. Spec. Publication, pp. 225–236.

De Rita, D., Cremisini, C., Cinnirella, A., Spaziani, F., 2011. Fluorine in the rocks and sediments of volcanic areas in central Italy: total content, enrichment and leaching processes and a hypothesis on the vulnerability of the related aquifers. Environ. Monit. Assess. http://dx.doi.org/10.1007/s10661-011-2381-3.

Deuser, W.G., Degens, E.T., 1967. Carbon isotope fractionation in the system CO_2 (gas)-CO_2 (aqueous)-HCO_3 (aqueous). Nature 215, 1033–1035.

Di Pippo, R., 2008. Binary cycle power plants. In: Butterworth-Heinemann (Ed.), Geothermal Power Plant: Principles, Applications, Case Studies and Environmental Impact, pp. 157–184. Amsterdam.

Doglioni, C., Gueguen, E., Harabaglia, P., Mongelli, F., 1999. On the origin of West directed subduction zones and applications to the western Mediterranean. In: Durand, B., et al. (Eds.), The Mediterranean Basins: Tertiary Extensions within the Alpine Orogen, vol. 156. Geol. Soc. Spec. Publ., pp. 541–561

Duchi, V., Minissale, A., 1995. Distribuzione delle manifestazioni gassose nel settore peritirrenico Tosco–Laziale e loro interazione con gli acquiferi superficiali. Boll. della Soc. Geol. Ital. 114, 337–351.

Duchi, V., Minissale, A., Paolieri, M., Prati, F., Valori, A., 1992. Chemical relationship between discharging fluids in the Siena-Radicofani graben and deep fluids produced by the geothermal fields of Mt. Amiata, Torre Alfina and Latera (central Italy). Geothermics 21, 401–413.

Dunai, T.J., Baur, H., 1995. Helium, neon, and argon systematics of the European subcontinental mantle: implications for its geochemical evolution. Geochim. Cosmochim. Acta 59, 2767–2783.

Etiope, G., 2015. Natural Gas Seepage. Springer International Publishing, Switzerland. http://dx.doi.org/10.1007/978-3-319-14601-0.

Fazzini, P., Gelmini, L., Mantovani, M.P., Pellegrini, M., 1972. Geologia dei monti della Tolfa (Lazio settentrionale; prov. di Viterbo e Roma). Mem. Soc. Geol. It. 11, 65–144.

Federico, C., Aiuppa, A., Allard, P., Bellomo, S., Jean-Baptiste, P., Parello, F., Valenza, M., 2002. Magma-derived gas influx and water-rock interactions in the volcanic aquifer of Mt. Vesuvius. Italy. Geochim. Cosmochim. Acta 66, 963–981.

Funiciello, R., Mariotti, G., Parotto, M., Preite-Martinez, M., Tecce, F., Toneatti, R., Turi, B., 1979. Geology, mineralogy and stable isotope geochemistry of the Cesano geothermal field (Sabatini Mountains, Northern Latium, Italy). Geothermics 8, 55–73.

Gambardella, B., Marini, L., Baneschi, I., 2005. Dissolved potassium in the shallow groundwaters circulating in the volcanic rocks of central-southern Italy. Appl. Geochem 20, 875–897.

Gat, J.R., Carmi, I., 1970. Evolution of the isotopic composition of atmospheric waters in the Mediterranean Sea area. J. Geophys. Res. 75, 3039–3048.

Giggenbach, W.F., 1980. Geothermal gas equilibria. Geochim. Cosmochim. Acta 44, 2021–2032.

Giggenbach, W.F., 1987. Redox processis governing the chemistry of fumarolic gas discharges from White Island. New Zeal. Appl. Geochem 2, 143–161.

Giggenbach, W.F., 1988. Geothermal solute equilibria. Derivation of Na-K-Ca-Mg geoindicators. Geochim. Cosmochim. Acta 52, 2749–2765.

Giggenbach, W.F., 1992. The composition of gases in geothermal and volcanic systems as a function of tectonic setting. Proc. Int. Symposium Water-Rock Interact. WRI-8 873–878.

Giggenbach, W.F., 1996. Chemical composition of volcanic gases. In: Scarpa, R., Tilling, R.I. (Eds.), Monitoring and Mitigation of Volcano Hazards. Springer, pp. 221–256.

Giggenbach, W.F., Goguel, R.L., 1989. Method for the Collection and Analysis of Geothermal and Volcanic Water and Gas Samples, vol. 2387, p. 53. NZ-DSIR Report, CD.

Honma, H., Itihara, Y., 1981. Distribution of ammonium in minerals of metamorphic and granitic rocks. Geochim. Cosmochim. Acta 13, 225–232.

Hooker, P.J., Bertrami, R., Lombardi, S., O'Nions, R.K., Oxburgh, E.R., 1985. Helium-3 anomalies and crust-mantle interaction in Italy. Geochim. Cosmochim. Acta 49, 2505–2513.

Javoy, M., Pineau, F., Allegre, C.J., 1982. Carbon geodynamic cycle. Nature 300, 171–173.

Karner, D.B., Marra, F., Renne, P.R., 2001. The history of the Monti Sabatini and Alban Hills volcanoes: groundwork for assessing volcanic-tectonic hazards for Rome. J. Volcanol. Geotherm. Res. 107, 185–219.

Longinelli, A., Selmo, E., 2003. Isotopic composition of precipitation in Italy: a first

overall map. J. Hydrol. 270, 75–88.

Machel, H.G., Krouse, H.R., Sassen, R., 1995. Products and distinguishing criteria of bacterial and thermochemical sulphate reduction. Appl. Geochem 10, 373–389.

Mamyrin, B.A., Tolstikhin, I.N., 1984. Helium Isotopes in Nature. Elsevier, Amsterdam.

Mango, F.D., 2001. Methane concentrations in natural gas: the genetic implications. Org. Geochem 32, 1283–1287.

Marini, L., Moretti, R., Accornero, M., 2011. Sulfur isotopes in magmatic-hydrothermal systems, melts, and magmas. Rev. Mineral. Geochem 73, 423–492.

Martelli, M., Nuccio, P.M., Stuart, F.M., Burgess, R., Ellam, R.M., Italiano, F., 2004. Helium-strontium isotope constraints on mantle evolution beneath the Roman Comagmatic Province. Italy. Earth Planet. Sci. Lett. 224, 295–308.

Martelli, M., Nuccio, P.M., Stuart, F.M., Di Liberto, V., Ellam, R.M., 2008. Constraints on mantle source and interactions from He-Sr isotope variation in Italian Plio-Quaternary volcanism. Geochem. Geophys 9. http://dx.doi.org/10.1029/2007GC001730.

Marty, B., 1995. Nitrogen content of the mantle inferred from N_2-Ar correlation in oceanic basalts. Nature 337, 326–328.

Marty, B., Jambon, A., 1987. C/^{3}He in volatile fluxes from the solid Earth: implications, for carbon geodynamics. Earth Planet. Sci. Lett. 83, 16–26.

McCollom, T.M., Seewald, J.S., 2007. Abiotic synthesis of organic compounds in deep-sea hydrothermal environments. Chem. Rev. 107, 382–401.

Mingram, B., Brauer, K., 2001. Ammonium concentration and nitrogen isotope composition in metasedimentary rocks from different tectonometamorphic units of the European Variscan Belt. Geochim. Cosmochim. Acta 65, 273–288.

Minissale, A., 2004. Origin, transport and discharge of CO_2 in Central Italy. Earth–Sci. Rev. 66, 89–141.

Minissale, A., Evans, W., Magro, G., Vaselli, O., 1997a. Multiple source components in gas manifestations from north–central Italy. Chem. Geol. 142, 175–192.

Minissale, A., Magro, G., Vaselli, O., Verrucchi, C., Perticone, I., 1997b. Geochemistry of waters and gas discharges from the Mt. Amiata silicic complex and surrounding areas (central Italy). J. Volcanol. Geotherm. Res. 79, 223–251.

Minissale, A., Vaselli, O., 2011. Karst springs as "natural" pluviometers: constraints on the isotopic composition of rainfall in the Apennines of central Italy. Appl. Geochem 26, 838–852.

Montegrossi, G., Tassi, F., Vaselli, O., Buccianti, A., Garofano, K., 2001. Sulfur species in volcanic gases. Anal. Chem. 73, 3709–3715.

Mook, W.G., Bommerson, J.C., Staverman, W.H., 1974. Carbon isotope fractionation between dissolved carbonate and gaseous carbon dioxide. Earth Planet. Sci. Lett. 22, 169–176.

Ohmoto, H., Rye, R.O., 1979. Isotopes of sulfur and carbon. In: Barnes, H.L. (Ed.), Geochemistry of Hydrothermal Ore Deposits, second ed. Wiley and Sons Ltd., Chichester, pp. 509–567.

O'Nions, R.K., Oxburgh, E.R., 1988. Helium volatile fluxes and the development of continental crust. Earth Planet. Sci. Lett. 90, 331–347.

Oppenheimer, C., Fischer, T.P., Scaillet, B., 2014. Volcanic Degassing: Process and Impact. In: Holland, H.D., et al. (Eds.). Elsevier, Pergamon, Oxford, pp. 111–179.

Ozima, M., Podosek, F.A., 2002. Noble gas Geochemistry, second ed. Cambridge University Press, Cambridge, UK, p. 286.

Parkhurst, D.L., Appelo, C.A.J., 2013. Description of input and examples for PHREEQC version 3-A computer program for speciation, batch-reaction, one-dimensional transport, and inverse geochemical calculations. U.S.G.S. Tech. Methods, book 6, chap. A43 497 available at: http://pubs.usgs.gov/tm/06/a43.

Peccerillo, A., 1985. Roman comagmatic province: evidence for subduction-related magma genesis. Geology 13, 103–106.

Peccerillo, A., 1999. Multiple mantle metasomatism in central-southern Italy: geochemical effects, timing and geodynamic implications. Geology 27, 315–318.

Polyak, B.G., Tolstikhin, I.N., 1985. Isotopic composition of the Earth's helium and the problem of tectonogenesis. Chem. Geol. 52, 9–33.

Poreda, R.J., Craig, H., 1989. Helium isotope ratios in circum-Pacific volcanic arcs. Nature 338, 473–478.

Procesi, M., Cantucci, B., Buttinelli, M., Armezzani, G., Quattrocchi, F., Boschi, E., 2013. Strategic use of the underground in an energy mix plan: synergies among CO_2, CH_4 geological storage and geothermal energy. Appl. Energy 110, 104–131.

Quigley, T.M., Mackenzie, A.S., 1988. The temperature of oil and gas formation in the sub-surface. Nature 333, 549–552.

Rizzo, A., Barberi, F., Carapezza, M.L., Di Piazza, A., Francalanci, L., Sortino, F., D'Alessandro, W., 2015. New mafic magma refilling a quiescent volcano; evidence from He-Ne-Ar isotopes during the 2011-2012 unrest at Santorini, Greece. Geochem. Geophys. Geosyst 16, 798–814.

Rollinson, H., 1993. Using Geochemical Data. Longman Group, London.

Rye, R.O., Bethke, P.M., Wasserman, M.D., 1992. The stable isotope geochemistry of acid sulphate alteration. Econ. Geol. Bull. Soc. 87, 225–261.

Sakai, H., 1968. Isotopic properties of sulfur compounds in hydrothermal processes. Geochim. J. 2, 29–49.

Salata, G.G., Roelke, L.A., Cifuentes, L.A., 2000. A rapid and precise method for measuring stable isotope ratios of dissolved inorganic carbon. Mar. Chem. 69, 153–161.

Sano, Y., Marty, B., 1995. Origin of carbon in fumarolic gas from island arcs. Chem. Geol. 119, 265–274.

Schoell, M., 1980. The hydrogen and carbon isotopic composition of methane from natural gases of various origins. Geochim. Cosmochim. Acta 44, 649–661.

Scrocca, D., Doglioni, C., Innocenti, F., 2003. Constraints for an interpretation of the Italian geodynamics: a review. Mem. Descr. Carta Geol. D'It 62, 15–46.

Takai, K., Nakamura, K., Toki, T., Tsunogai, U., Miyazaki, M., Miyazaki, J., Hirayama, H., Nakagawa, S., Nunoura, T., Horikoshi, K., 2008. Cell proliferation at 122°C and isotopically heavy CH_4 production by a hyperthermophilic methanogene under high-pressure cultivation. PNAS 105, 10949—10954.

Tang, Y., Perry, J.K., Jenden, P.D., Schoell, M., 2000. Mathematical modeling of stable carbon isotope ratios in natural gases. Geochim. Cosmochim. Acta 64, 2673—2687.

Taran, Y.A., 2005. A method for determination of the gas-water ratio in bubbling springs. Geophys. Res. Lett. 32, L23403. http://dx.doi.org/10.1029/2005GL024547.

Tassi, F., Fiebig, J., Vaselli, O., Nocentini, M., 2012. Origins of methane discharging from volcanic-hydrothermal, geothermal and cold emissions in Italy. Chem. Geol. 310—311, 36—48.

Tedesco, D., Allard, P., Sano, Y., Wakita, H., Pece, R., 1990. Helium-3 in subaerial and submarine fumaroles of Campi Flegrei caldera. Italy. Geochim. Cosmochim. Acta 54, 1105—1116.

Tedesco, D., 1997. Systematic variations of ^{3}He/^{4}He ratios and carbon of fumarolic fluids from active volcanic areas of Italy: evidence of radiogenic ^{4}He and crustal carbon addition by the subductiong African plate? Earth Planet. Sci. Lett. 151, 255—269.

Thode, H.G., 1991. Sulphur isotope in nature and the environment: an overview. In: Krouse, H.R., Grinenko, V.A. (Eds.), Stable Isotopes — Natural and Anthropogenic Sulphur in the Environment. Scope 43. Wiley, Chichester, pp. 1—23.

Vaselli, O., Tassi, F., Montegrossi, G., Capaccioni, B., Giannini, L., 2006. Sampling and analysis of volcanic gases. Acta Volcanol. 18, 65—76.

Whitfield, M., 1978. Activity coefficients in natural waters. In: Pytkowicz, R.M. (Ed.), Activity Coefficients in Electrolyte Solutions. CRC Press, Boca Raton, FL, pp. 153—300.

Whiticar, M.J., 1999. Carbon and hydrogen isotope systematics of bacterial formation and oxidation of methane. Chem. Geol. 161, 291—314.

Whiticar, M.J., Faber, E., Schoell, M., 1986. Biogenic methane formation in marine and freshwater environments: CO_2 reduction vs. acetate fermentation — isotopic evidence. Geochim. Cosmochim. Acta 50, 693—709.

Worden, R.H., Smalley, P.C., 1996. H_2S-producing reactions in deep carbonate gas reservoirs: khuff Formation. Abu Dhabi. Chem. Geol. 133, 157—171.

Zhang, J., Quay, P.D., Wilbur, D.O., 1995. Carbon isotope fractionation during gas-water exchange and dissolution of CO_2. Geochim. Cosmochim. Acta 82, 161—173.

Zuppi, G.M., Fontes, J.C., Letolle, R., 1974. Isotopes du milieu et circulation d'eaux sulfurées dans le Latium. In: Isotope Techniques in Groundwater Hydrology, vol. 1. IAEA, Vienna, pp. 341—361.